MODELING OF CHLORINE DISINFECTION AND KAOLIN DISPERSION SYSTEMS WITH CONTROL APPLICATIONS

By

FERIDUN DEMIR

A DISSERTATION PRESENTED TO THE GRADUATE SCHOOL OF THE UNIVERSITY OF FLORIDA IN PARTIAL FULFILLEMENT OF THE REQUIREMENTS FOR THE DEGREE OF DOCTOR OF PHILOSOPHY

UNIVERSITY OF FLORIDA

2001

"To my family"

Feridun DEMIR

ACKNOWLEDGMENTS

I would like to express my sincere appreciation to Dr. Oscar D. Crisalle and Dr. Spyros A. Svoronos for their excellent guidance, assistance and advice on the control part of my dissertation; Dr. Abbas A. Zaman on the colloidal dispersions studies.

I would to thank Dr. Ben L. Koopman and Dr. Gar B. Hoflund for their willingness to serve on my supervisory committee, and for their valuable suggestions. I would like to thank all of the Chemical Engineering Department and Engineering Research Center of Particle Science and Technology, University of Florida, faculty and personnel for their help and cooperation.

I would like to thank the Kanapaha Water Reclamation Facility and the University of Florida Wastewater Treatment Plant personnel. I would like to thank the Vinings Industries Inc. and Engelhard Corporation for funding and for supplying materials during my research. Finally, I also would like to thank all my friends in Chemical Engineering and ERC for their help and cooperation. Special thanks are to due to Wilbur W. Woo, who helped me to develop some of key equations used in the simulation studies for the wastewater treatment plant.

My studies at the University of Florida were supported by a fellowship from the Turkish Government. I am grateful for this support.

TABLE OF CONTENTS

page

ACKNOWLEDGMENTS iii

LIST OF TABLES vii

LIST OF FIGURES viii

ABSTRACT xii

CHAPTERS

1 INTRODUCTION 1

1.1 Introduction 1
1.2 Wastewater Disinfection 3
1.2.1 Chlorine 3
1.2.2 Ozone 4
1.2.3 Ultraviolet Radiation 5
1.3 Kaolinite (Pure Kaolin) 6
1.4 Conclusions 8

2 KINETIC MODELS OF DISINFECTION 9

2.1 Introduction 9
2.2 Chlorination 9
2.3 Models of Disinfection 11
2.4 Method of Characteristics (MC) 13
2.5 Dynamic Model for Disinfection 14
2.6 Conclusions 20

3 PROCESS CONTROL STRATEGIES FOR DISINFECTION 21

3.1 Introduction 21
3.2 Control Difficulties of Disinfection 21
3.2.1 Large Delay 21
3.2.2 Disturbances 22
3.3 Cascade Control 22
3.4 Dead Time Compensation 24

3.5 Conclusions 27

4 MODIFIED SMITH PREDICTOR (DEAD TIME COMPANSATION) USING THE ODOMETRIC TRANSFORMATION 29

4.1 Introduction 29
4.2 The Odometric Variable 29
4.3 Modified Smith Predictor 30
4.4 Open Loop Simulation Study 33
4.5 Closed Loop Simulation Study 47
4.6 Conclusions 51

5 DISSOLUTION CAPACITY OF METAL IONS FROM CRUDE KAOLIN PARTICLES IN THE ABSENCE AND THE PRESENCE OF ANIONIC DISPERSING AGENTS 52

5.1 Introduction 52
5.2 Materials and Methods 53
5.2.1 Materials 53
5.2.2 Sample Preparation 55
5.2.3 Chemical Analysis 55
5.3 Dissolution Capacity of Metal Ions 57
5.3.1 Effect of Solids Concentration in the Absence of Dispersing Agents 57
5.3.2 Effect of the Dosage of Disparsant without pH Adjustment 59
5.3.3 Effect of %Solid (WT) in the Presence of Dispersants without pH Adjustment 64
5.3.4 Effect of pH 67
5.4 Dissolution Capacity of Metal Ions using Design of Experiment (DOE) Software 70
5.4.1 Effect of pH Modifiers on Solubility of Metal Ions 70
5.4.2 Effect of Dispersing Agents on Solubility of Aluminum Ions 73
5.4.3 Effect of Dispersing Agents on Solubility of Silicon Ions 82
5.5 Predictive Models for the Concentration of Aluminum and Silicon Ions in the Presence of Dispersing Agents 89
5.6 Conclusions 95

6 SUMMARY AND CONCLUSIONS 96

7 SUGGESTIONS FOR FUTURE WORK 98

APPENDIX

A SIMULATION PROGRAM FOR ODOMETRIC TRANSFORMATION USING MATLAB 100

B OPEN LOOP SIMULATION PROGRAM USING VISUAL BASIC 113

C CLOSED LOOP SIMULATION PROGRAM USING VISUAL BASIC 118

LIST OF REFERENCES 123

BIOGRAPHICAL SKETCH 126

LIST OF TABLES

page

Table

1-1 Advantages and disadvantages of disinfection methods 8

4-1 Process parameters obtained from open loop simulation program ($\Delta t = 0.5$ sec)... 42

4-2 Process parameters obtained from open loop simulation program ($\Delta t = 5$ sec)..... 42

4-3 Process parameters obtained from open loop simulation program ($\Delta t = 10$ sec).... 42

4-4 Process parameters obtained from open loop simulation program ($\Delta t = 20$ sec).... 42

5-1 Chemical composition of Georgia Crude Kaolin 56

5-2 Dissolved aluminum and silicon ion concentrations from Georgia Crude kaolin under various experimental conditions in the presence of NaPAA using NaOH and Na_2CO_3 as pH modifiers..... 72

5-3 Factors and levels for experimental design using Box Behnken method..... 74

5-4 Complete and the best linear quadratic regression models for the dissolution of aluminum ions from kaolin in the presence of different dispersing agents 93

5-5 Complete and the best linear regression models for the dissolution of silicon ions from kaolin in the presence of different dispersing agents..... 94

LIST OF FIGURES

page

Figure

2-1 Method of characteristic 13

2-2 Odometric transformation 15

2-3 The method of characteristic applied to a concentration field 16

2-4 Simulation results at $k_{Slow} = 0.0080\ h^{-1}$ 17

2-5 Simulation results at $k_{Slow} = 0.0075\ h^{-1}$ 18

2-6 Simulation results at $k_{Slow} = 0.0070\ h^{-1}$ 18

2-7 Simulation results at $k_{Slow} = 0.0074\ h^{-1}$ 19

2-8 Simulation results at $k_{Slow} = 0.0073\ h^{-1}$ 19

2-9 Simulation results at $k_{Slow} = 0.0072\ h^{-1}$ 20

3-1 Block diagram of cascade control 23

3-2 Feedback system with the Smith Predictor 26

3-3 The Smith Predictor with approximate $G'(s)$ and D' 27

4-1 Cascade control diagram of the wastewater treatment plant 31

4-2 Smith Predictor scheme for the master controller 31

4-3 Simulation results ($\Delta t = 0.5$ sec, Reactor number = 50) 35

4-4 Simulation results ($\Delta t = 0.5$ sec, Reactor number = 100) 35

4-5 Simulation results ($\Delta t = 0.5$ sec, Reactor number = 500) 36

4-6 Simulation results ($\Delta t = 0.5$ sec, Reactor number = 1000) 36

4-7 Simulation results ($\Delta t = 5$ sec, Reactor number = 50) 37

4-8 Simulation results (Δt = 5 sec, Reactor number = 100) 37

4-9 ... Simulation results (Δt = 5 sec, Reactor number = 200) 38

4-10 Simulation results (Δt = 5 sec, Reactor number = 300) 38

4-11 Simulation results (Δt = 10 sec, Reactor number = 50) 39

4-12 Simulation results (Δt = 10 sec, Reactor number = 100) 39

4-13 Simulation results (Δt = 10 sec, Reactor number = 150) 40

4-14 Simulation results (Δt = 20 sec, Reactor number = 50) 40

4-15 Simulation results (Δt = 20 sec, Reactor number = 90) 41

4-16 Process parameters obtained from open loop program (Δt = 0.5 sec)..... 43

4-17 Process parameters obtained from open loop program (Δt = 5 sec)..... 44

4-18 Process parameters obtained from open loop program (Δt = 10 sec)..... 45

4-19 Process parameters obtained from open loop program (Δt = 20 sec)..... 46

4-20 Variation of flow rate with time 47

4-21 Simulation result (K_{gain} = 0.06155, Reactor num. = 500, τ = 10, Δt = 0.5 sec, D = 85)..... 49

4-22 Simulation result (K_{gain} = 0.06215, Reactor num. = 200, τ = 10, Δt = 5 sec, D = 85)..... 49

4-23 Simulation result (K_{gain} = 0.06225, Reactor num. = 100, τ = 16, Δt = 10 sec, D = 81)..... 50

4-24 Simulation result (K_{gain} = 0.06231, Reactor num. = 50, τ = 22, Δt = 20 sec, D = 79) 50

5-1 Kaolin particles..... 54

5-2 Concentration of aluminum and silicon ions from kaolin particles in the absence of dispersing agents 58

5-3 Concentration of Al^{3+} as a function of dispersants dosage in the supernatant at fixed level of 55%solids (wt) 61

5-4 Concentration of Si^{4+} as a function of the dispersants dosage in the supernatant at fixed level of 55 %solids (wt) 62

5-5 Variation of pH in the dispersions at the various dosage of dispersants at fixed level of 55%solids (wt) 63

5-6 Concentration of Al^{3+} as a function of %solids (wt) in the supernatant using three dispersing agents a dosage level of 5 65

5-7 Concentration of Si^{4+} as a function of %solids (wt) in the supernatant using three dispersing agents a dosage level of 5 66

5-8 Concentration of metal ions as a function of pH from kaolin at fixed level of solid concentration (35 %solids (wt)) in the absence of dispersant 69

5-9 Surface response plot for the effects of pH and NaPAA dosage on solubility of aluminum from kaolin (time = 13 hrs, %solids (wt) = 35) 75

5-10 Contour plots for the effects of pH and NaPAA dosage on solubility of aluminum from kaolin (time = 13 hrs, %solids (wt) = 35) 76

5-11 Interaction graph for the effects of NaPAA and pH on solubility of aluminum from kaolin (time = 13 hrs, %solids (wt) = 35)..... 77

5-12 Surface response plot for the effects of pH and NaHMP dosage on solubility of aluminum from kaolin (time = 13 hrs, %solids (wt) = 35) 78

5-13 Contour plots for the effects of pH and NaHMP dosage on solubility of aluminum from kaolin (time = 13 hrs, %solids (wt) =35) 79

5-14 Surface response plot for the effects of pH and Na-Silicate dosage on solubility of aluminum from kaolin (time = 13 hrs, %solids (wt) = 35) 80

5-15 Contour plots for the effects of pH and Na-Silicate dosage on solubility of aluminum from kaolin (time = 13 hrs, %solids (wt) = 35) 81

5-16 Surface response plot for the effects of pH and NaPAA dosage on solubility of silicon from kaolin (time = 13 hrs, %solids (wt) = 35)..... 83

5-17 Contour plots for the effects of pH and NaPAA dosage on solubility of silicon from kaolin (time = 13 hrs, %solids (wt)= 35)..... 84

5-18 Surface response plot for the effects of pH and NaHMP dosage on solubility of silicon from kaolin (time = 13 hrs, %solids (wt) = 35) 85

5-19 Contour plots for the effects of pH and NaHMP dosage on solubility of silicon from kaolin (time = 13 hrs, %solids (wt)= 35) 86

5-20 Surface response plot for the effects of pH and Na-Silicate dosage on solubility of silicon from kaolin (time = 13 hrs, %solids (wt) = 35) 87

5-21 Contour plots for the effects of pH and Na-Silicate dosage on solubility of silicon from kaolin (time = 13 hrs, %solids (wt) = 35) 88

5-22 Residuals versus predicted values for the effect of NaPAA dosage on solubility of aluminum from kaolin particles 91

5-23 Predicted versus observed values for the effect of NaPAA dosage on solubility of aluminum from kaolin particles 92

Abstract of Dissertation Presented to the Graduate School
of the University of Florida in Partial Fulfillment of the
Requirements for the Degree of Doctor of Philosophy

MODELING OF CHROLINE DISINFECTION AND KAOLIN DISPERSION SYSTEMS WITH CONTROL APPLICATIONS

By

Feridun Demir

December 2001

Chairman: Dr. Oscar D. Crisalle, Cochairman: Dr. Abbas A. Zaman
Major Department: Chemical Engineering

This dissertation presents an analysis of a chlorine disinfection process and on a kaolin dispersion process with the goals of developing models and additional insight that would be ultimately useful for the purpose of designing effective automatic control schemes. The chlorine disinfection study focuses on the fact that the large contact times required for effective wastewater treatment involve a large and variable time-delay which in turn makes the design of a control system more challenging. This monograph uses a plug-flow reactor model to represent the dynamics of the process, resulting in a partial differential equation. It is shown that the method of characteristics can be used to reduce the model to an ordinary differential equation which still captures the key dynamic features of the original model but that is more amenable to analysis using conventional process control techniques. Finally, an odometric transformation is introduced to take advantage of the fact that the variations in time delay are introduced exclusively by changes in flow rate. The odometrically-transformed model features a constant dead time

that is shown to be equal to the length of the reactor. It is also shown that the constant-delay transformed model can be used as the basis for the design of a Smith Predictor scheme for time delay compensation, which is free from the undesirable performance degradation typically observed when the time delay varies. Preliminary closed-loop simulation studies suggest that effective control of the chlorine disinfection process could be achieved using a cascade control scheme coupled with a modified Smith Predictor master controller designed using the odometrically transformed process.

In the kaolin dispersion study the effect of pH and three different anionic dispersants (sodium polyacrylate, sodium hexametaphosphate and sodium silicate) were investigated on the dissolution capacity of metal ions from kaolin particles. The dosage of dispersing agent, pH, solid concentration and aging significantly affected the solubility of metal ion concentrations. Released aluminum ions precipitated as $Al(OH)_3$ with increasing and decreasing suspension pH. Analogously, increasing the pH of the suspension results in the formation of alumino-silicate surface on the silica surface of particles, and this situation prohibited the release of silicon ions from the kaolin particles. Some of the aluminum ions adsorbed onto the surface of released silicon ions, and formed alumino-silicate gel. The complete and best models were obtained for the dissolution of aluminum and silicon ions from kaolin particles. These models are useful for future designs of appropriate controllers to maintain the surface properties of kaolin at a desired value.

CHAPTER 1
INTRODUCTION

1.1 Introduction

The process of chlorine disinfection of wastewater and the colloidal properties of kaolin dispersion were investigated with the objective of developing models useful for designing appropriate controllers. The basic goal of wastewater disinfection is to supply healthy, usable water by killing disease-causing microorganisms. In order to understand the significance of disinfection, we should recognize that disinfection is the last process available to kill disease-causing microorganisms before wastewater is discharged. As the population increases, so does the demand for fresh water. Wastewater can be a very significant water source if it is reused efficiently. The disinfection process supplies usable water and also protects the environment from harmful microorganisms. Many disinfection processes have been developed. These include application of heat, light, oxidizing chemicals, acids and alkalis, metal ions, and surface-active chemicals (Grasso, 1996). The selection of a disinfection process for wastewater treatment requires many considerations. These considerations should be made based on cost, ability to kill certain microorganisms, controllability, and the corrosive properties of the disinfectant. Plant size, operation and maintenance service, and transportation and storage of the disinfectant are other consideration factors. Chlorination, ozonation, and UV radiation are very reasonable processes for wastewater treatment after considering these factors.

Kaolin is used as coating and filling agent in many industries such as paper, rubber, plastics, ceramics and paint (Murray, 2000). The paper industry is the largest industry that uses kaolin. It utilizes about the 50 percent of the kaolin production, while 10 percent is used in refractories, and 10 percent is used in pottery (Van Olphen, 1991). It is applied as fillers and as coatings in papers. When it is used as a filler, the paper becomes more homogenous in texture and is more suitable for printing. When it is applied as a coating agent, the papers become brighter and gloss (Van Olphen, 1991). In the paper industry finer kaolin particles are usually used, typically with a particle size less than 2 μm (Kendall, 1995). The main objective of the kaolin industry is to prepare dispersion at high solids concentration and to keep the rheological behavior at a desired condition during the process. To spread the kaolin dispersion as a thin layer on the paper, low viscosity and high solids concentrations are necessary. To prepare well-dispersed suspension at high solids concentration, some dispersing agents must be added, usually phosphates and anionic dispersing agents (Van Olphen, 1991). The adsorption of dispersing agents onto the surface of kaolin particle changes the rheological behavior of the dispersion and produces a well-dispersed suspension. When the dispersing agents are used, the solubility of metal ions, mainly aluminum and silicon ions, from the surface of kaolin particles increases. Many researchers believe that there is a relationship between the soluble salt concentration and the rehological behavior of the suspension. The solubility of metal ions from kaolin particles is also strongly related to the pH of the suspension (Huertas et al. 1998, Huertas et al. 1999, and Ganor et al. 1995). In this document the adsorption of dispersing agents onto the kaolin particles, the dissolution capacity of aluminum and silicon, and the effect of pH on the solubility of aluminum and

silicon ions are investigated. The resulting models are useful for the future design of a controller.

Wastewater Disinfection

1.2.1 Chlorine

One of the most important steps in wastewater treatment is disinfection of the effluent before it is discharged. Chlorine is the most widely used chemical for disinfection. It has been used as a disinfectant since 1908 to protect public health. The effectiveness of chlorine depends on the chlorine demand of the water, the time that chlorine is in contact with the organisms, and the water quality. Specifically, the following behavior is observed (Grasso, 1996 and Reed, 1998).

- When the concentration of chlorine increases, the required contact time for disinfection decreases.
- When the water's pH increases, the effectiveness of chlorine disinfection decreases.
- If there is turbidity in the water, the effectiveness of chlorine disinfection decreases.
- When chlorine is added to the water, it also reacts with other substances in the stream, including iron, manganese, hydrogen sulfide, and ammonia. In a typical wastewater treatment plant, there is an especially large amount of ammonia. In order to achieve disinfection successfully, more chlorine should be added than is required for chemical reactions. The amount of chlorine that reacts with chemicals plus the amount required for disinfection is called the chlorine demand of the water.

When chlorine is added to water or wastewater, hydrolysis occurs and then a mixture of hypochlorous acid (HOCl) and hydrochloric acid (HCl) is formed. The reaction depends on both temperature and pH. Hypochlorous acid is a weak acid and it dissociates in water to form a solution of hypochlorite ions (OCl^-). When the pH is higher than 8.5, hypochlorous acid dissociates to form H^+ and OCl^-, which are dominant ions. When the pH is lower than 6.0, hypochlorous acid does not dissociate and remains

dominant at the equilibrium point (Grasso, 1996). The key chemical reactions are (Grasso, 1996)

$$Cl_2(g) + H_2O \leftrightarrow HOCl + H^+ + Cl^- \quad (1.1)$$

$$HOCl \leftrightarrow H^+ + OCl^- \quad (1.2)$$

Wastewater includes large amounts of ammonia. Chlorine reacts with ammonia to form chloramines (mono-, di-, and trichloramines) or combined chlorines. Organic nitrogen also reacts with chlorine to form organochloramines. Because of the significance of disinfection using chlorine and its use at the Kanapaha Water Reclamation Facility (KWRF), which is the focus of this research project, more details are given in Chapter 2 of this document.

1.2.2 Ozone

Ozone is an unstable gas when it is dissolved in water. Ozone inactivates bacteria by totally or partially destroying the cell wall (Grasso, 1996). However, the disinfection mechanism of ozone is not well understood. Ozone disinfection is made either from direct ozone oxidation of the microorganism or from the reaction of radical byproducts formed during ozone decomposition (Grasso, 1996). Since ozone disinfection is affected only slightly by pH, the disinfection mechanism is thought to result from direct ozone oxidation.

Ozone disinfection is considered to be an alternative to chlorine disinfection for wastewater treatment. Unlike chlorine disinfection, there are no taste, odor and color problems associated with ozone use. However, ozone is more expensive than chlorine. It is a very powerful chemical oxidizing agent and must be used immediately, because of storage difficulties.

As mentioned earlier, the process of disinfection with ozone is not fully understood. Some researchers suggest that it destroys viral proteins so that invasion of a susceptible cell is prohibited. The attack of ozone on purines and dipyramidines found in nucleic acids results in addition of OH and hydrogen across the double bonds, opening of the rings, or formation of thymine dimers. Ozone also breaks nitrogen-carbon bonds between sugars and affects the DNA structure by breaking hydrogen bonds (Grasso, 1996). One study showed that the primary reaction mechanism with the unsaturated fatty acids of the phospholipids, glycoproteins, and glycolipids in the cell membrane, resulted in leakage of cellular constituents outside the cell (Grasso, 1996).

1.2.3 Ultraviolet Radiation

Ultraviolet (UV) disinfection is another alternative to chlorine disinfection. Disinfection with UV inactivates microorganisms by damaging cellular nucleic acids, the molecular subunits of DNA (Grasso, 1996). When UV damages bacterial DNA, the bacteria cannot reproduce. Ultraviolet disinfection differs from chlorination and ozonation. The concentrated UV light inactivates the pathogens by hindering their ability to replicate, as opposed to destruction as in the case of oxidation. The genetic material of microorganisms absorbs UV, and then pyrimidine dimers are formed and join neighboring cytosine or thymine moieties by a cyclobutane ring. These dimers are the major cause of the lethal and mutagenic effects of UV radiation (Grasso, 1996).

The optimum wavelength of UV light to achieve disinfection is usually between 250 and 265 nm. This is based on the maximum absorption spectrum for nucleic acids. The UV disinfection method is very simple. Lamps producing UV light are placed at a controlled liquid depth in an open channel. When the wastewater passes through the

channel, the pathogenic microorganisms are exposed to UV light. In order to achieve disinfection successfully, the required exposure time ranges from six to ten minutes. Typical UV setup systems are (Lau, 1997):

- Low-pressure, low-intensity systems
- Low-pressure, medium-intensity systems
- Medium-pressure, high-intensity systems

The term "low-pressure" refers to a pressure of mercury in the UV lamp of approximately 10^{-2} torr. The term "low-intensity" means that the lamp power is around 65 watts (Lau, 1997).

Each disinfection method has many advantages and disadvantages yet all of them are being used successfully.

1.3 Kaolinite (Pure Kaolin)

Kaolin is widely used in industry and new applications for it are found continuously. It is primarily used in paper, paint, rubber, plastics, ceramic, cosmetic products, and dyes. In the paper industry, it is used as a filling and coating component to improve paper quality such as smoothing the surface of paper, brightness, opacity and printability of paper (Konta, 1995). It is also used in the plastics industry in applications such as plastic covers, foils, water pipes, tubes, and cables. The particle size range of kaolin is also important for industrial applications (Konta 1995).

Kaolinite, which has the chemical composition $Si_2Al_2O_5(OH)_4$ consists of one octahedral alumina and one tetrahedral silica sheet, is a 1:1 pure clay mineral (Weaver and Pollard, 1973). Octahedral and tetrahedral sheets are formed as $(SiO_4)^{4-}$ and $(AlO_3(OH)_3)^{6-}$ ions (Konta, 1995). These sheets share one of four oxygen of the

tetrahedral silica sheet and they form one layer kaolinite mineral. These layers are attached together through hydrogen bonding and each particle approximately consists of 50 alternating layers. The aspect ratio of kaolin particles, which are plate-like in shape, may vary from 5 to 15, depending on the mechanical treatment of the particles (Sjoberg et al. 1999).

There is a significant charge difference between the basal plane and the edge of the particles. As a result of this difference, an electrostatic edge-to-face attraction forms a card-house type of agglomerate that coagulates the suspension (Herrington et al. 1992). When the charge of the suspension is increased using an alkali substance beyond the Iso Electric Point (IEP) of alumina, the edge is covered by negative charges, and because of the electrostatic repulsion, particles start to repel each other and a well-dispersed suspension is produced (Herrington et al. 1992).

The fluidity of a kaolin dispersion is a significant problem when it is used in industry. Especially in paper coating, the solids concentration of kaolin dispersion can usually be as high as 60% or 70% solids (wt), and it must be well dispersed, have a stable viscosity, and good flow characteristics for processibility (Sjoberg et al. 1999).

In order to obtain the dispersion at desired conditions, some dispersing agents must be added. Kaolinite is a hydrophilic material and can be dispersed in water by adding selected dispersing agents (Murray, 2000). These dispersing agents can be anionic electrolytes, polyelectrolytes, or surfactants, and they usually adsorb on the kaolin particles and make the particles negatively charged. These negatively charged particles repel each other because of electrostatic or electrosteric forces and increase the fluidity of the dispersion.

1.4 Conclusion

Specific advantages and disadvantages of each method are shown in Table 1-1.

Table 1-1. Advantages and disadvantages of disinfection methods

Disinfection Method	Advantages	Disadvantages
Chlorination	Provides residual disinfectant Can be used for many water problems (bacteria, metal ions, etc.) Inexpensive Can disinfect large volume of water Requires low electricity Well known technology Easily meets disinfection standards	Requires long contact time Gives chlorine taste Can form THMs Not very effective at low level Difficult to store Can be effected by turbidity Residuals can be toxic to the environment
Ozonation	Does not have residual toxicity Does not form THMs Can disinfect large volumes of water Is not effected by pH Can kill almost all pathogens Does not require long contact time (between two and ten minutes)	More expensive than chlorine Requires a high degree of maintenance Requires an extra chamber Requires cooling water Requires special storage
Ultraviolet radiation	Does not change the taste of water Easy to use Does not require long contact time Easy to design Well known technology	Requires high electricity Does not have residual effect Requires pretreatment for turbidity Requires special cleaning and renovation of lamp manually

CHAPTER 2
KINETIC MODELS OF DISINFECTION

2.1 Introduction

The three most common disinfection methods were discussed in Chapter 1. As explained, each method has many advantages and disadvantages. Chlorination is the most widely applied disinfection method used today. The Kanapaha Water Reclamation Facility (KWRF) in Gainesville, Florida, uses chlorine as its only disinfection method. In this chapter, the kinetics of the disinfection mechanisms for a wastewater stream presented in the literature are reviewed. In addition, a plug-flow reactor model is presented to describe the dynamics of a wastewater treatment plant. A solution of the partial differential equations of plug-flow model is pursued using the well known "Method of Characteristics" (MC), which yields an equivalent set of ordinary differential equations and hence makes the solution much easier.

2.2 Chlorination

Chlorine is a greenish-yellow gas. Its molecular weight is 35.453 g/mole and is a member of the halogen group (Grasso, 1996, and Tchobanoglous, 1985). It is heavier than air in the gas form, and heavier than water in the liquid form. It reacts with many elements and compounds. When it is applied to water, it is highly soluble, even at the room temperature, and reacts with water to give the following reactions (Hammer, 1996):

$$Cl_2(g) + H_2O \leftrightarrow HOCl + H^+ + Cl^- \quad (2.1)$$

$$HOCl \leftrightarrow H^+ + OCl^- \quad (2.2)$$

These reactions are pH dependent. When the pH is higher than 8.5, the acid dissociates to form H^+ and OCl^-, which become the dominant species, and when the pH is less than 6.0, the system remains as a solution of HOCl, which is dominant at the equilibrium point (Grasso, 1996).

Ammonia-nitrogen compounds are usually present in wastewater in the form of ammonia gas (NH_3), ammonium ions (NH^+), or nitrogen-containing organic compounds. Chloramines are produced, when an aqueous solution of chlorine contacts any form of ammonium-nitrogen. As long as chlorine is added, all amine-nitrogens react with chlorine and its hydrogen is replaced by chlorine, and eventually nitrogen gas is released (Tchobanoglous, 1985). These chloramine reactions are as follows:

$$HOCl + NH_3 \leftrightarrow NH_2Cl \text{ (monochloramine)} + H_2O$$

$$HOCl + NH_2Cl \leftrightarrow NHCl_2 \text{ (dichloramine)} + H_2O$$

$$HOCl + NHCl_2 \leftrightarrow NCl_3 \text{ (nitrogen trichlorde)} + H_2O \qquad (2.3)$$

Further addition of chlorine results in free chlorine residuals. This chlorination is called *breakpoint chlorination.* In order to understand it, four steps should be considered during chlorination. Recall that there are some chemical substances (Fe^{+2}, H_2S) and ammonia-nitrogen in the wastewater treatment plant. In the first step, when chlorine is added to wastewater, it reacts with chemical substances and is reduced to chloride. In the next step, if chlorine addition is maintained, chloramines and chloroorganic compounds are formed. In the third step, when we continue the addition of chlorine, the chlorine starts to react with chloramines and other chloroorganic compounds and produces N_2O, chloride, and N_2. These reactions are as follows:

$$NH_2Cl + NHCl_2 + HOCl \leftrightarrow N_2 + 4HCl$$

$$2NH_2Cl + HOCl \leftrightarrow N_2 + H_2O + 3HCl \quad (2.4)$$

At this point, which is called the breakpoint, almost all chloramines and chloroorganic compounds are completely oxidized, and further addition of chlorine results in free chlorine residuals (Tchobanoglous, 1985).

2.3 Models of Disinfection

The chlorination reactions can be modeled based on breakpoint chlorination reactions in a wastewater treatment plant. Morris and Wei, (1969) modeled these reactions for eight species as follows:

$$HOCl + NH_3 \rightarrow NH_2Cl + H_2O$$

$$HOCl + NH_2Cl \rightarrow NHCl_2 + H_2O$$

$$HOCl + NHCl_2 \rightarrow NCl_3 + H_2O$$

$$NCl_3 + H_2O \rightarrow HOCl + NHCl_2$$

$$NHCl_2 + H_2O \rightarrow NOH + 2H^+ + 2Cl^-$$

$$NOH + NH_2Cl \rightarrow N_2 + H_2O + H^+ + Cl^-$$

$$NOH + NHCl_2 \rightarrow N_2 + HOCl + H^+ + Cl^-$$

$$NOH + 2HOCl \rightarrow NO_3^- + 3H^+ + 2Cl^- \quad (2.5)$$

Saunier (1978) proposed the following reaction rate expressions for these reactions:

$$r_{HOCl} = - k_1[HOCl][NH_3] - k_2[HOCl][NH_2Cl] - k_3[HOCl][NHCl_2] + k_4[NCl_3] + k_7[NOH][NHCl_2] - 2k_8[HOCl][NOH] - k_{Slow}[HOCl]$$

$$r_{NH3} = - k_1[HOCl][NH_3]$$

$$r_{NH2Cl} = k_1[HOCl][NH_3] - k_2[HOCl][NH_2Cl] - k_6[NH_2Cl][NOH]$$

$$r_{NHCl2} = k_2[HOCl][NH_2Cl] - k_3[HOCl][NHCl_2] + k_4[NCl_3]$$

$$k_5[NHCl_2] - k_7[NOH][NHCl_2]$$

$$r_{NCl3} = k_3[HOCl][NHCl_2] - k_4[NCl_3]$$

$$r_{NOH} = k_5[NHCl_2] - k_6[NH_2Cl][NOH] - k_7[NOH][NHCl_2]$$

$$- k_8[HOCl]^2[NOH] \qquad (2.6)$$

where $k_1, k_2, \ldots, k_8$ are kinetic rate constants. The term $k_{Slow}[HOCl]$ represents the chlorine consumption by disinfection (Anastassiadis, 1994). We viewed that process as a pseudo first-order reaction.

Saunier (1979) developed the following expression for the reaction rate constants for chlorination reactions, showing the explicit dependence on pH and temperature:

$$k_1 = 9.7 \cdot 10^8 e^{-3.0/RT_K}$$

$$k_2 = 1.99 \cdot 10^4 e^{-2.4/RT_K}$$

$$k_3 = 3.43 \cdot 10^5 e^{-7.0/RT_K}\left(1 + \frac{10^{-pK_a+1.4}}{[H^+]}\right)$$

$$k_4 = 8.56 \cdot 10^8 e^{-18.0/RT_K}\left(1 + 5.88 \cdot 10^5 [OH^-]\right)$$

$$k_5 = 2.03 \cdot 10^{14} e^{-7.2/RT_K} n_1 [OH^-]$$

$$k_6 = 10^8 e^{-6.0/RT_K}$$

$$k_7 = 1.3 \cdot 10^9 e^{-6.0/RT_K}$$

$$k_8 = 10^7 e^{-6.0/RT_K} \qquad (2.7)$$

where T_K is absolute temperature, R is ideal gas constant, and n_1 is the initial ammonia concentration ($n_1 = [NH_3] + [NH_4^+]$). Saunier (1979) developed a model for the HOCl hydrolysis constant (K_a) of the form

$$pK_a = \frac{3000}{T_K} - 10.0686 + 0.0253T_K \qquad (2.8)$$

where $pK_a = -\log K_a$

2.4 Method of Characteristics (MC)

The method of characteristics is a technique used to solve a partial differential equation (PDE) by reducing it to a set of ordinary differential equations (ODEs). In accomplish, independent variables of the PDE should be transformed to new variables. It is best to explain the method using the general expression for a PDE

$$Pp + Qq = Pz_x + Qz_y = R(x, y) \tag{2.9}$$

where P and Q are constants, z_x and z_y are derivatives of z with respect to variables respectively, and R can be a function of x and y. The constants P and Q define a characteristic line that makes an angle

$$\theta = \tan^{-1}\left(\frac{Q}{P}\right) \tag{2.10}$$

with the x-axis (see Figure 2-1).

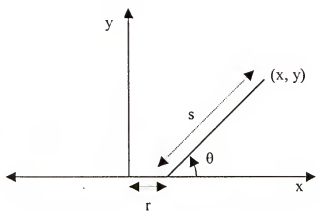

Figure 2-1. Method of Characteristics

Let

$$x = r + s\cos(\theta) \tag{2.11a}$$

$$y = s\sin(\theta) \tag{2.11b}$$

where r and s are variables whose geometric interpretation is given in Figure 2.1. After substituting Equations 2.11a and 2.11b into Equation 2.9 and integrating to solve the PDE yields

$$z(x,y) = z(x - y\cot\theta) + \int_0^{\operatorname{cosec}\theta} R(x - y\cot\theta + s'\cos\theta, s'\sin\theta)\frac{ds'}{\sqrt{P^2 + Q^2}} \qquad (2.12)$$

Finally, this equation can be transformed to an ODE by taking the derivative with respect to the variable s.

2.5 Dynamic Model for Disinfection

The model of chlorination disinfection reactor considered is based on a material balance, and the assumption that the dynamic is described by a plug flow behavior. The other key assumptions are that no diffusion exists in the direction of flow and that the cross-sectional area is constant. These assumptions result in a first-order partial differential equation for each of eight species. Namely

$$\frac{\partial c_i}{\partial t} = -v(t)\frac{\partial c_i}{\partial z} + r_i(\underline{c}(t,z)) \qquad (2.13)$$

where $i = 1, 2, \ldots, 8$, and c_i is the concentration of species i, z is the location along the length of the reactor, t is the time variable, v is the linear flow velocity, and $\underline{c}$ is a vector whose components are the compositions c_i. The model (2.13) was investigated by Anastassiadis (1994).

An important concern is the presence of a large and highly variable time-delay, which reduces the control performance and effluent quality. The time-delay varies as a function of the flow rate of wastewater. An odometric transformation is then introduced to transform the dynamics of the system to constant time-delay model an equivalent. The odometric transformation replaces time with a new variable, the displacement of flow. If

we let β be the cumulative distance traveled by water, the mathematical representation of this transformation becomes

$$\frac{\partial \beta}{\partial t} = v(t) \tag{2.14}$$

The odometric transformation, shown in Equation (2.14), has been proposed and used in analogizes context by Harmon et al (1990) and by Svoronos and Lyberotos (1992). Substituting this into Equation (2.13) yields

$$\frac{\partial c_i}{\partial \beta} = -\frac{\partial c_i}{\partial z} + \frac{1}{v(\beta)} r_i\left(\underline{c}(\beta, z)\right) \tag{2.15}$$

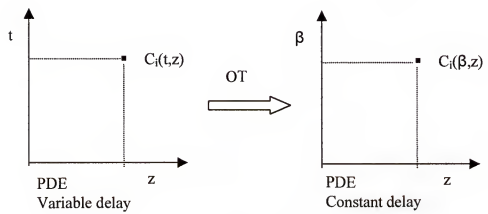

Figure 2-2. Odometric transformation

Figure 2-3 shows the odometric transformation substitution schematically. Equation (2.15) is a first-order PDE with constant delay, which is independent of time. Furthermore, the coefficients of $\partial c_i/\partial z$ and $\partial c_i/\partial \beta$ are constants and equal to 1. Applying the method of characteristics discussed in Section 2.3 and using the equivalencies, shown in Figure 2-3, gives the first-order ODE.

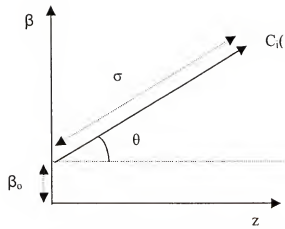

Figure 2-3. The method of characteristics applied to a concentration field.

$$\frac{\partial c_i\left(\beta_o + \frac{\sigma}{\sqrt{2}}, \frac{\sigma}{\sqrt{2}}\right)}{\partial \sigma} = \frac{1}{\sqrt{2}} \frac{1}{v\left(\beta_o + \frac{\sigma}{\sqrt{2}}\right)} r_i\left(\underline{c}\left(\beta_o + \frac{\sigma}{\sqrt{2}}, \frac{\sigma}{\sqrt{2}}\right)\right) \tag{2.16}$$

Measurements of chlorine concentrations were taken at KWRF to solve Equation (2.16). Measurements were taken at the chlorination point, at the beginning of the first contact basin and at the end of second contact basin. A step change was made at the chlorination point, and its effect was observed along the whole reactor. Measurements of ammonia concentration could not be taken successfully. Therefore, in order to eliminate chemical reactions with ammonia, we assumed that the disinfection reaction is a pseudo first-order reaction at all points located between the first and the second contact basin. We used the chlorine measurement at the beginning of the first contact basin for the simulation. Simulation results and experimental results are shown in Figures 2-4 through 2-9. The figures show the measured chlorine concentration at the first basin (solid line). This probe is also known as the north probe. The figure also shows the chlorine concentration measured at the final probe (dashed line). Finally, the figures include the simulation results (black circles) that were obtained for a first order chlorine consumption

reactor with kinetic rate constant k_{Slow}. The different figures were obtained using trial values of k_{Slow}. The results suggest that a value of $k_{Slow} = 0.0072\ h^{-1}$ (see Figure 2.9) yields good agreement with the experimental data.

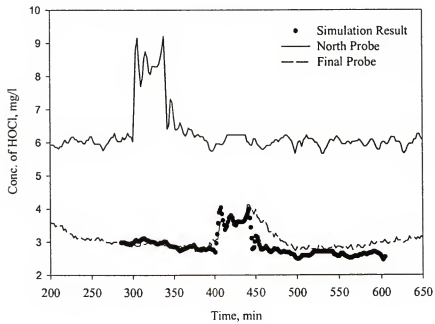

Figure 2-4. Simulation results at $k_{Slow} = 0.0080\ h^{-1}$

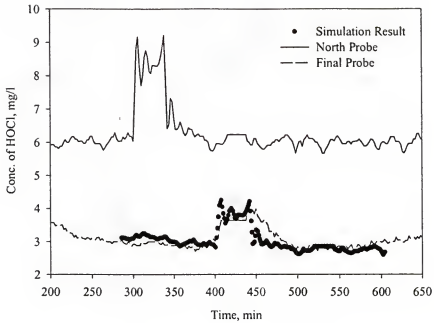

Figure 2-5. Simulation results at $k_{Slow} = 0.0075\ h^{-1}$

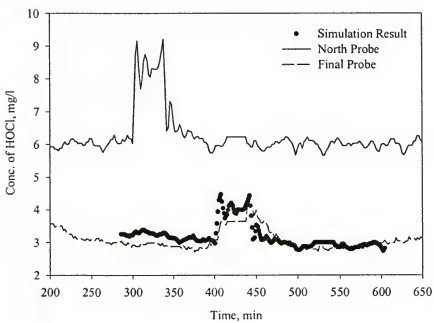

Figure 2-6. Simulation results at $k_{Slow} = 0.0070\ h^{-1}$

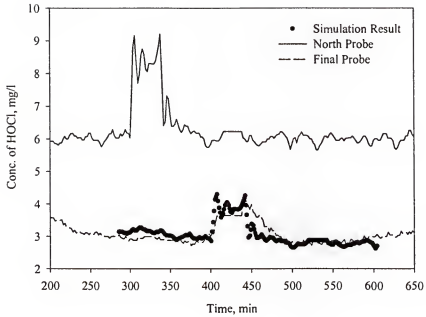

Figure 2-7. Simulation results at $k_{Slow} = 0.0074\ h^{-1}$

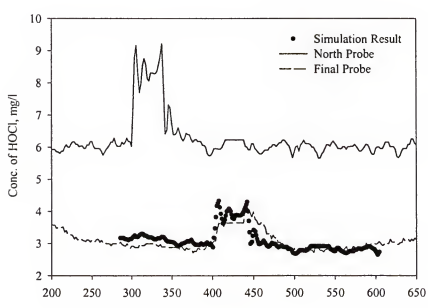

Figure 2-8. Simulation results at $k_{Slow} = 0.0073\ h^{-1}$

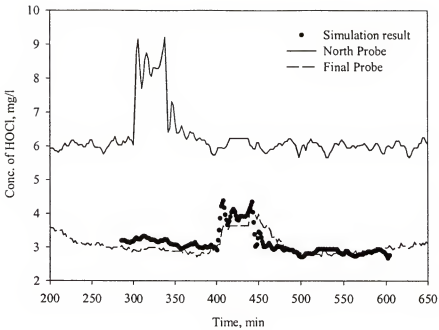

Figure 2-9. Simulation results at $k_{Slow} = 0.0072\ h^{-1}$

2.6 Conclusion

An odometric transformation and the method of characteristics were used to transform a PDE model with varying dead time to an ODE model with constant dead time. The resulting model is easier to analyze. It was also shown that a first-order kinetic model is able to describe well the chlorine consumption in the ammonia-free part of the contact basin.

CHAPTER 3
PROCESS CONTROL STRATEGIES FOR DISINFECTION

3.1 Introduction

The objective of this chapter is to develop a control strategy for the disinfection process of a wastewater treatment plant. A major problem with the disinfection process is the presence of large and variable transportation lags. The desired objective of the disinfection is to produce effluent that meets required environmental regulations at the end of the reactor. For example, the Kanapaha Water Reclamation Facility (KWRF) must discharge effluent with a total chlorine residual of more than 1 mg/L (Anastassiadis, 1994).

In order to disinfect the treated wastewater well and avoid the formation of organic compounds known as trihalomethanes, just enough chlorine must be added. The treated wastewater leaving KWRF must meet the requirement of the State of Florida standards. Feedback control of the chlorination process is necessary to meet requirements. It doses the minimum chlorine amount for disinfection and avoids very high chlorine concentration that causes the formation of trihalomethanes.

3.2 Control Difficulties in Disinfection

3.2.1 Large Delay

The presence of a time delay (DT) in the control loop complicates the design and weakness the stability of an on-line controller. The presence of a time delay reduces the quality of control due to unavoidable reduction in the control gains (Levine, 1996). If the

transfer function includes time delay, it means that the characteristic equation includes the term e^{-Ds}, hence it is more difficult to check the stability than the standard case of a polynomial equation (Chu et al. 1998).

3.2.2 Disturbances

Disturbances are variables that affect the output but are not adjusted by the process operator or automatically. Some disturbances in the KWRF include the effect of sunlight, rainfall, etc. Sunlight affects the chlorine chemistry due to UV radiation, eliminating chlorine molecules and hence reducing the final chlorine residual (Levine, 1996). Rainfall also reduces the chlorine concentration by dilution and affects the chlorine residuals at the end of the contact basin.

3.3 Cascade Control

Cascade control is usually applied when there is one control variable and more than one measured variable. It is also useful if there are long dead times or long time constants between the control variable and process variable (Marlin, 1995). In order to obtain fast responses to the control variable, intermediate feedback control loops are used. There are two loops in a cascade control configuration. One of them is called the primary loop. The measured variable of the primary control loop is the measured variable that we are interested in. The manipulated variable of the primary control loop is the set point of the secondary loop that adjusts the process input. The secondary loop gives faster responses since the time delay is small. In order to improve the performance, more than one control loop can be added (Marlin, 1995 and Seborg, 1989). The basic cascade control diagram is shown in Figure 3-1 (Anastassiadis, 1994). Transfer functions can be derived from this diagram for the relation between the control variable $y_1(s)$ and

the input variable of the primary loop $u_1(s)$, and the measurement variable of the secondary loop $y_2(s)$ and the input variable of the secondary loop $u_2(s)$, as follows:

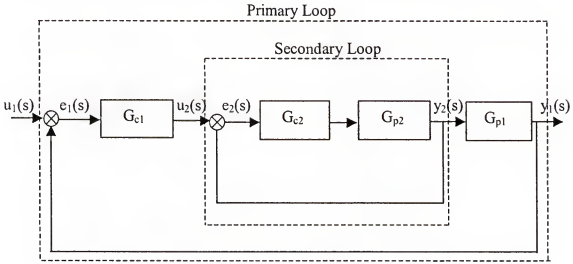

Figure 3-1. Block diagram of cascade control

$$G_2(s) = \frac{G_{c2}(s)G_{p2}(s)}{1 + G_{c2}(s)G_{p2}(s)} \tag{3.1}$$

$$G_1(s) = \frac{G_{c1}(s)G_2(s)G_{p1}(s)}{1 + G_{c1}(s)G_2(s)G_{p1}(s)} \tag{3.2}$$

where

G_{c_1}=Primary controller transfer function

G_{p_1}=Primary process transfer function

G_{c_2}=Secondary controller transfer function

G_{p_2}=Secondary controller transfer function

The best way to introduce the cascade control is to explain it using as an example our chlorination reactor. The goal of the cascade control scheme is to maintain the exit free-chlorine residual concentration at a certain level, as required by environmental regulations. Hence, the exit free-chlorine residual concentration is the control variable of

the primary loop. There is a very large time delay between this control variable and the process input, which is the chlorine dosage added at the beginning of the reactor. This time delay usually varies between two to three hours. At the beginning of the reactor there is chemical reaction between ammonia and chlorine. This reduces the free-chlorine residual concentration significantly. Ammonia reacts with the free chlorine very fast and is consumed completely at the beginning of the reactor. The disinfection process takes place at the rest of the reactor. In addition to the disinfection process, there are some external disturbances that also effect the free chlorine residual concentration. The chemical reaction with ammonia also affects the control variable. In order to decrease its affect, the secondary loop is added. The set point of the secondary loop is the controller output of the primary loop. This secondary loop uses the primary controller output and adjusts the process input, which is the chlorine added to the process. The secondary loop is basically the manipulated variable of the primary loop. The net feedback effect is the same for single loop or cascade control. The single-loop configuration connot deliver good control for this process because there is a very large time delay. In contrast, the cascade control is expected to deliver better performance.

3.4 Dead Time Compensation

The primary loop of the cascade control structure has a significant time delay at the wastewater chlorination process in the Kanapaha Water Reclamation Facility. This time delay is approximately equal to two or three hours, and it also varies with time as the flow rate changes. Consequently the feedback control loop does not give good performance. In order to increase the performance for systems with constant time delay, one may use the Smith Predictor, which is also known as Dead Time Compensator

(Stefanopoulos, 1984). The purpose of the Smith Predictor is to cancel the dead time and obtain a transfer function that is delay-free. The basic block diagram of the Smith Predictor is shown in Figure 3-2 (Stefanopoulos, 1984).

In order to discuss the Smith Predictor, lets assume that the feedback loop has a controller $G_c(s)$, and a process transfer function G(s) with dead-time e^{-Ds}, shown in Figure 3.2 (a). The open loop response for this system is

$$\bar{y}(s)=G_c(s)G(s)e^{-Ds}\bar{y}(s)_{sp} \tag{3.3}$$

which clearly displays the dead time. Introducing the signals

$$\bar{y}'(s)=(1-e^{-Ds})G_c(s)G(s)\bar{y}(s)_{sp} \tag{3.3}$$

and

$$\bar{y}'(s)=\bar{y}'(s)+\bar{y}(s) \tag{3.4}$$

as shown in Figure 3-2 (b), the net effect is a closed loop that is delay-free, as shown in Figure 3-2 (c) (Stefanopoulos, 1984).

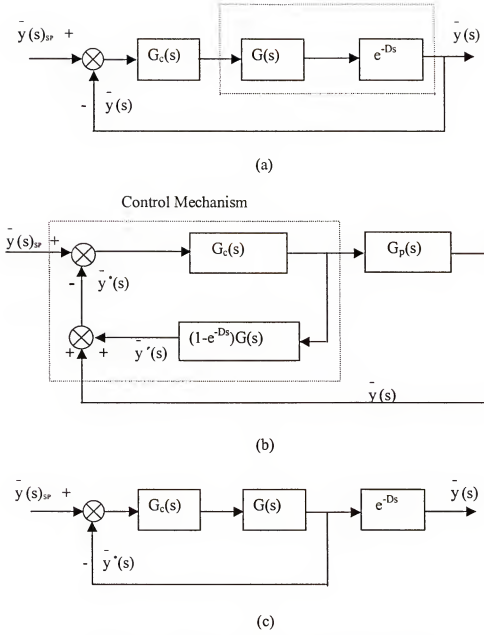

Figure 3-2. Feedback system with the Smith Predictor

In reality the model of the process and the dead time are not known perfectly. Assuming that G(s) and e^{-Ds} represent the correct models of the process, we use the notation $G^*(s)$ and $e^{-D's}$ to represent the approximate respective models. Using this nomenclature, the dead-time compensator adopts the form shown in Figure 3-3.

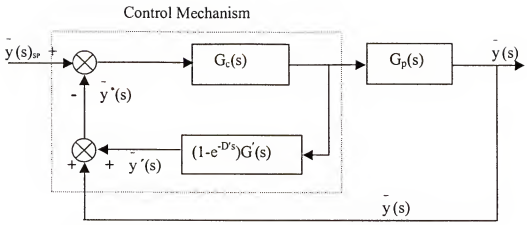

Figure 3-3. The Smith Predictor with approximate $G'(s)$ and D'

If the exact model G(s) and D are not respectively equal to the approximate models $G'(s)$ and D', the signal $\bar{y}^*$ becomes

$$\bar{y}^*(s) = G_c(s)(G'(s) + (G(s)e^{-Ds} - G'(s)e^{-D's}))G'(s)\bar{y}(s)_{SP} \qquad (3.5)$$

This equation shows that when there is mismatch between the model and the real process, the compensation is not effective, because the delay does not cancel out.

Clearly, effective time-delay compensation requires that the delay be a constant. If that is not the case, the Smith Predictor will fail to cancel out the delay. We are able to use the Smith Predictor for our project because the odometric transformation discussed in Section 4.2 permits transforming the model to a constant-delay system.

3.5 Conclusion

Cascade control and Dead Time Compensation are two advanced control strategies that hold good potential for successful control performance. The cascade control scheme features a secondary (or slave) controller whose probe is located in proximity of the dosage point; hence it is affected by a small time delay and it can therefore be tuned efficiently. The other controller in the cascade is a primary (or master) controller that adjusts the set point of the slave controller. The master is affected by a

large and variable dead time; however, using an odometric transformation, the reactor model can be written as a constant dead time system. The Smith Predictor is then used to design an effective dead time compensation for the master controller.

CHAPTER 4
MODIFIED SMITH PREDICTOR (DEAD TIME COMPANSATION) USING THE ODOMETRIC TRANSFORMATION

4.1 Introduction

Chapter 3 discusses how the feedback scheme could be made delay-free using dead time compensation if the delay happens to be constant. Large and variable dead time values, however, prevent the use of a standard dead time compensation scheme for the disinfection of wastewater. Since the contact basin is very long and the flow rate of wastewater changes daily, the delay of the process is in fact large and variable.

The model of the system is also very important in terms of control performance. The odometric transformation mentioned in Section 4.2 can be used to transform the dynamics of the system to constant time-delay model (Harmon et al. 1990; Svoronos and Lyberatos, 1992). It replaces time with a new variable, β, which is the displacement of flow. The method of characteristics is then used to transform the constant-delay partial differential equations (PDEs) into ordinary differential equations (ODEs). The resulting equations were then coded in VISUAL BASIC for simulation purposes.

4.2 The Odometric Variable

The large and highly variable time-delay is a main challenge for the Wastewater reclamation technology. The time-delay varies with the inlet flow rate of wastewater. The odometric transformation discussed in Section 4.2 can be used to transform the dynamics of the system to a constant time-delay model (Harmon et al., 1990; Svoronos and Lyberatos, 1992). The odometric transformation replaces time with a new variable,

β, which is interpreted as the cumulative distance traveled by water. Hence, the mathematical representation of the odometric transformation becomes

$$\frac{\partial \beta}{\partial t} = v(t) \tag{4.1}$$

The advantage of new variable β is that it leads to a constant delay, which in term is equal to the length of the contact basin. The constant delay can be used to design an effective Smith Predictor for the master control loop.

4.3 Modified Smith Predictor

Cascade control and dead-time compensation strategies were applied to develop an effective control strategy. Figures 4-1 and 4-2 show the relevant diagrams for the control schemes proposed. The cascade control structure of Figure 4-1 features a slave controller whose probe is located close to the dosage point; hence this loop is affected by a small time delay and it can therefore be tuned tightly. The master controller adjusts the set point of the slave controller. In contrast, The master is affected by a large and variable dead time; however, using an odometric transformation, the reactor model can be written as a constant dead time system. The Smith Predictor is then used to design an effective dead time compensation for the master controller. The resulting master control configuration is shown in Figure 4.2, where the master controller consists of a PID controller within a Smith Predictor scheme. The process G_p shown in Figure 4-2 represents the slave closed-loop, i.e., it includes the slave PI controller and the dosage-response variable y_1. The process block G shown inside the Smith Predictor block in Figure 4-2 is a linear approximation to the process G_p, and the block G_c represents a PID master controller.

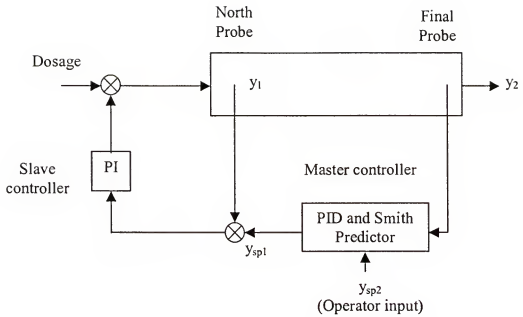

Figure 4-1. Cascade control diagram for the wastewater treatment plant

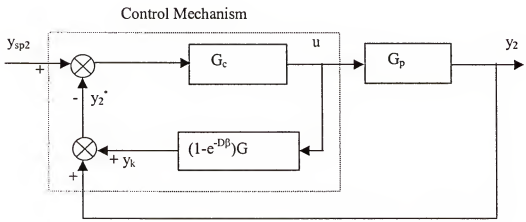

Figure 4-2. Smith Predictor scheme for the master controller

In terms of the odometric variable (β), the set point for the slave controller is

$$u(\beta) = y_{sp1}(\beta) \tag{4.2}$$

where u(β) is the output of the master controller (see Figures 4-1 and 4.2).

The design of the Smith Predictor operator G in Figure 4-2 is based on first-order plus dead-time approximation to the slave loop dynamics in the β domain (rather than on the time-domain). We introduce the discrete increment of the odometric variable

$$\Delta\beta = \frac{D}{N} \tag{4.3}$$

where N is the number of discrete basins that approximate the plug-flow reactor, and D is the length of the reactor. Then, a discrete version of the signal y_k produced by the Smith Predictor block in Figure 4-2 is given by recursive expression

$$y_k(\beta) = (1 - \frac{\Delta\beta}{\tau})y_k(\beta - \Delta\beta) + K_{gain}\left[u(\beta - \Delta\beta) - u(\beta - D - \Delta\beta)\right]\frac{\Delta\beta}{\tau} \tag{4.4}$$

It follows that

$$y_2^*(\beta) = y_2(\beta) + (1 - \frac{\Delta\beta}{\tau})y_k(\beta - \Delta\beta) + K_{gain}\left[u(\beta - \Delta\beta) - u(\beta - D - \Delta\beta)\right]\frac{\Delta\beta}{\tau} \tag{4.5}$$

where $y_2(\beta)$ is measured by the final probe. Let the feedback error for the master loop be

$$e(\beta) = y_{sp2}(\beta) - y_2^*(\beta) \tag{4.6}$$

then the velocity form of the discrete control law for the master PID controller G_c in Figure 4-2 is

$$u(\beta) = u(\beta - \Delta\beta) + K_c\left[e(\beta) - e(\beta - \Delta\beta) + \frac{\Delta\beta}{\tau_I}e(\beta) + \frac{\tau_D}{\Delta\beta}(e(\beta) - 2e(\beta - \Delta\beta) + e(\beta - 2\Delta\beta))\right] \tag{4.7}$$

where

y_1 = north probe reading

y_2 = final probe reading

y_{sp1} = set point of slave loop

y_{sp2} = set point of the master loop

D = delay (length of reactor)

K_{gain} = gain of slave closed-loop of process

β = odometric transformation variable

N = number of reactors used to approximate the plug-flow reactor

$u(\beta)$ = manipulated output of master loop

y_k = intermediate signal in the Smith Predictor scheme

K_c = gain of the master controller

τ_I = integral time constant of the master controller

τ_D = derivative time constant of the master controller

Finally, the control law (4.7) is used in conjunction with the relationship (4.2) to configure the complete cascade control system shown in Figure 4-1.

4.4 Open Loop Simulation Study

The closed-loop controls Equations (4.2) through (4.7) were coded in a VISUAL BASIC program. The flow rate of wastewater, residence time, and rate constant of the disinfection reactor were obtained experimentally from the University of Florida wastewater treatment plant. First, an open-loop version of the simulation program was run to find the apparent process parameters, namely the process gain (K_{gain}), the time constant (τ), and the Delay (D). The contact basin was assumed to behave as a plug-flow reactor described by Equation (2.26), which was solved by approximating the reactor small with N continously-stired-tank reactors. For modeling purposes, an adequate number of N reactors was calculated by running the open-loop simulation program. More specifically, various time increments (Δt) were used for integrating the equations,

namely, 0.5, 5, 10, and 20 sec, and the corresponding reactor numbers and process parameters were calculated. The results of fitting a first order plus delay models to the step response data yields experimental values of apparent process gain (K_{gain}), time constant (τ) and Delay (D) (Stefanopoulos, 1984). The results are shown in Tables 4-1 to 4-4 for different step sizes. Then results are plotted in Figures 4-3 to 4-19 as a function of the integration step size. The final probe values shown in the figures are deviations from the steady state values of 2.8 mg/L. Therefore, a deviation value of 0 mg/L in the Figures 4-3 to 4-19 corresponds to an actual measurement of 2.8 mg/L. Likewise, a deviation value of 1 mg/L read from the figures corresponds to an actual value of 3.8 mg/L.

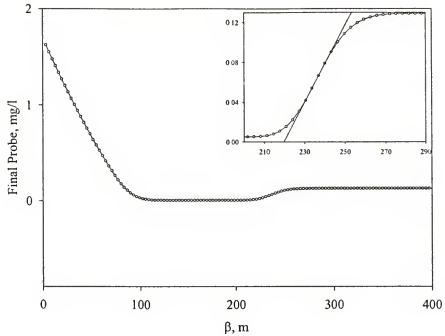

Figure 4-3. Simulation results (Δt = 0.5 sec, Reactor number = 50)

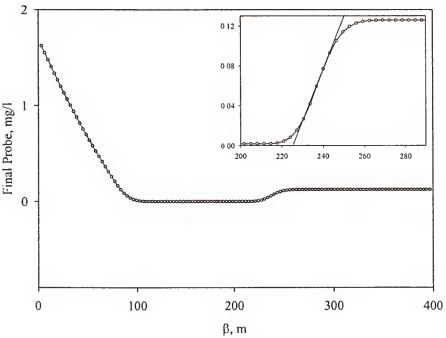

Figure 4-4. Simulation results (Δt = 0.5 sec, Reactor number = 100)

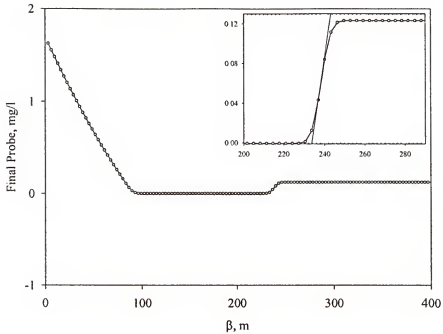

Figure 4-5. Simulation results ($\Delta t = 0.5$ sec, Reactor number = 500)

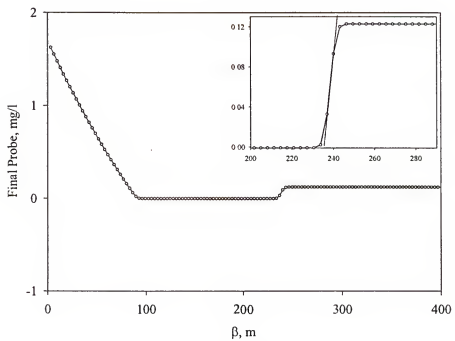

Figure 4-6. Simulation results ($\Delta t = 0.5$ sec, Reactor number = 1000)

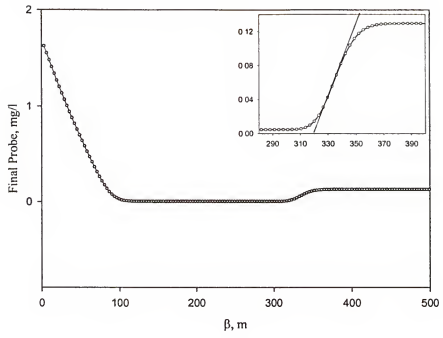

Figure 4-7. Simulation results (Δt = 5 sec, Reactor number = 50)

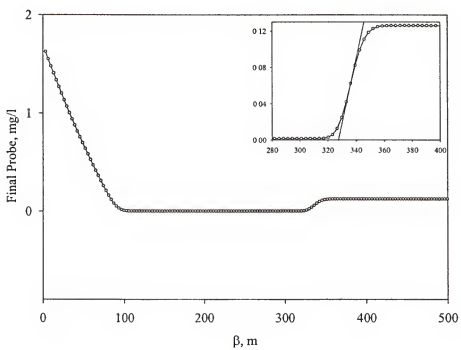

Figure 4-8. Simulation results (Δt = 5 sec, Reactor number = 100)

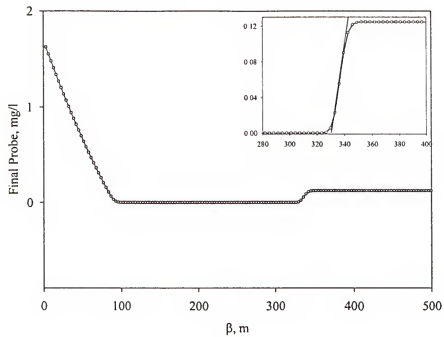

Figure 4-9. Simulation results (Δt = 5 sec, Reactor number = 200)

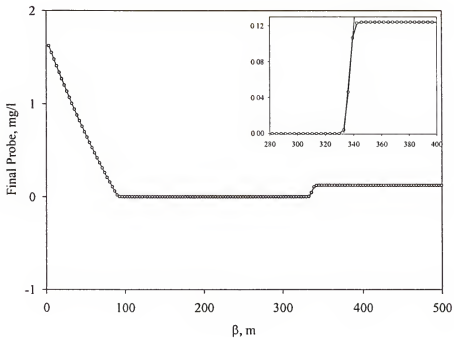

Figure 4-10. Simulation results (Δt = 5 sec, Reactor number = 300)

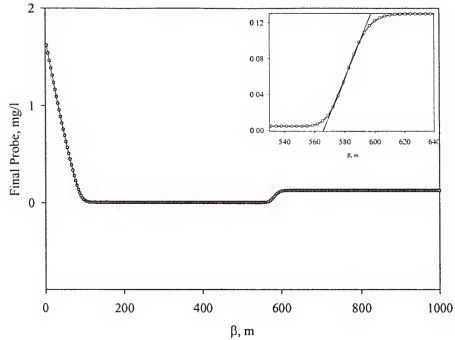

Figure 4-11. Simulation results (Δt = 10 sec, Reactor number = 50)

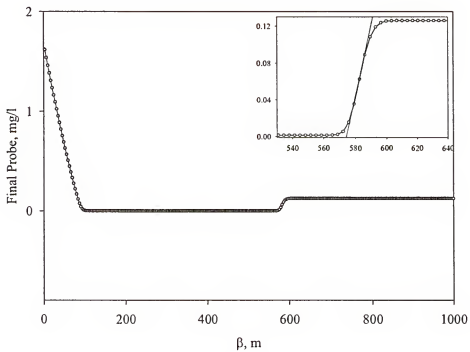

Figure 4-12. Simulation results (Δt = 10 sec, Reactor number = 100)

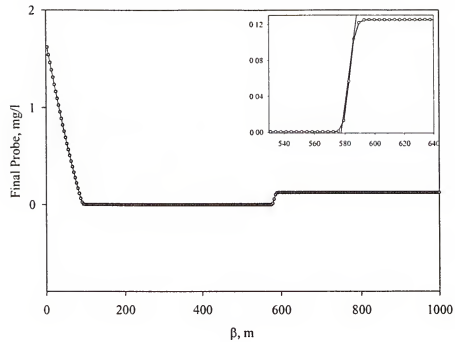

Figure 4-13. Simulation results (Δt = 10 sec, Reactor number = 150)

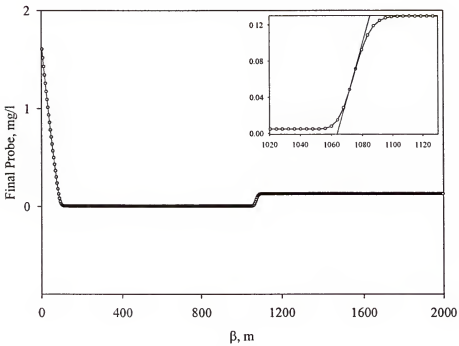

Figure 4-14. Simulation results (Δt = 20 sec, Reactor number = 50)

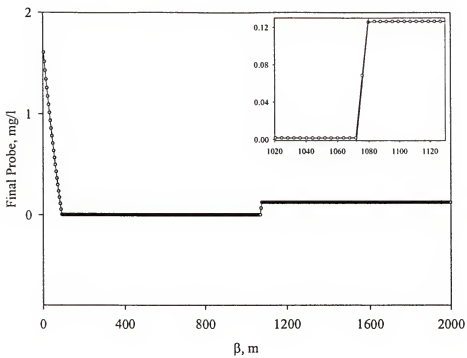

Figure 4-15. Simulation results ($\Delta t = 20$ sec, Reactor number = 90)

Table 4-1. Process parameters obtained from open loop simulation program ($\Delta t = 0.5$ sec)

Reactor Number	Process Gain, K_{gain}	τ (m)	D (m)
50	0.061696	33	72
100	0.061366	21	80
500	0.061555	10	85
1000	0.061420	7	87

Table 4-2. Process parameters obtained from open loop simulation program ($\Delta t = 5$ sec)

Reactor Number	Process Gain, K_{gain}	τ (m)	D (m)
50	0.061785	32	73
100	0.062154	19	80
200	0.06220	10	85
300	0.062153	7	87

Table 4-3. Process parameters obtained from open loop simulation program ($\Delta t = 10$ sec)

Reactor Number	Process Gain, K_{gain}	τ (m)	D (m)
50	0.062066	29	74
100	0.062247	16	81
150	0.062231	8	86

Table 4-4. Process parameters obtained from open loop simulation program ($\Delta t = 20$ sec)

Reactor Number	Process Gain, K_{gain}	τ (m)	D (m)
50	0.062314	22	79
90	0.062267	7	87

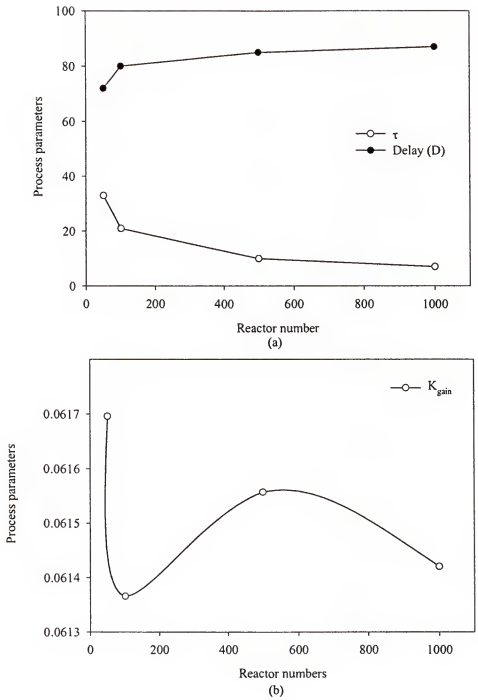

Figure 4-16. Process parameters obtained from open loop program ($\Delta t = 0.5$ sec)

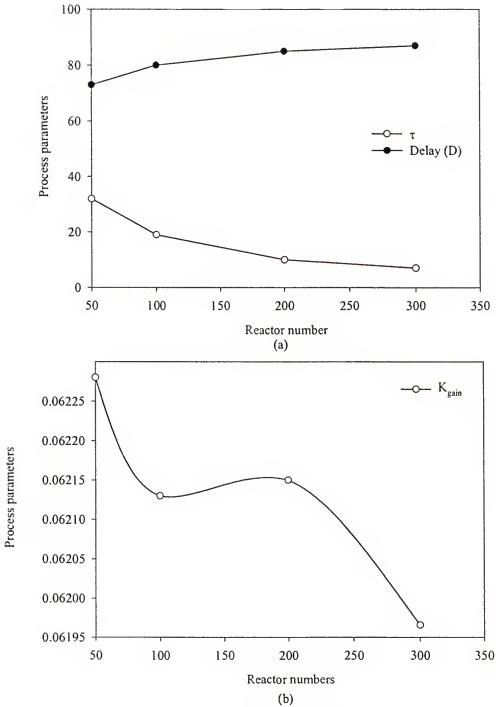

Figure 4-17. Process parameters obtained from open loop program ($\Delta t = 5$ sec)

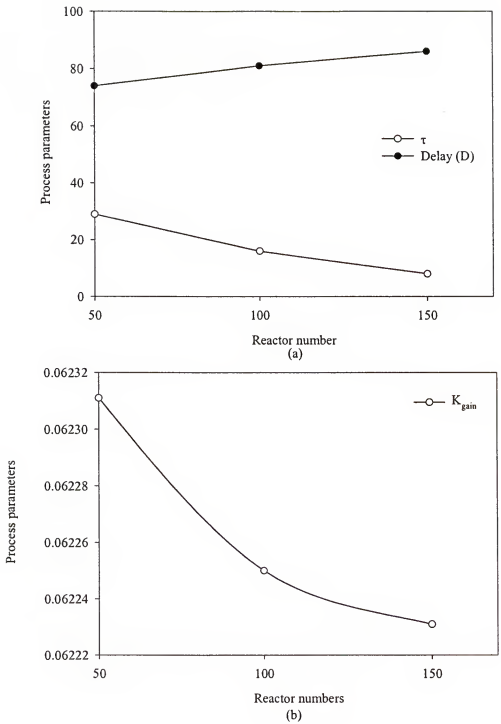

Figure 4-18. Process parameters obtained from open loop program (Δt = 10 sec)

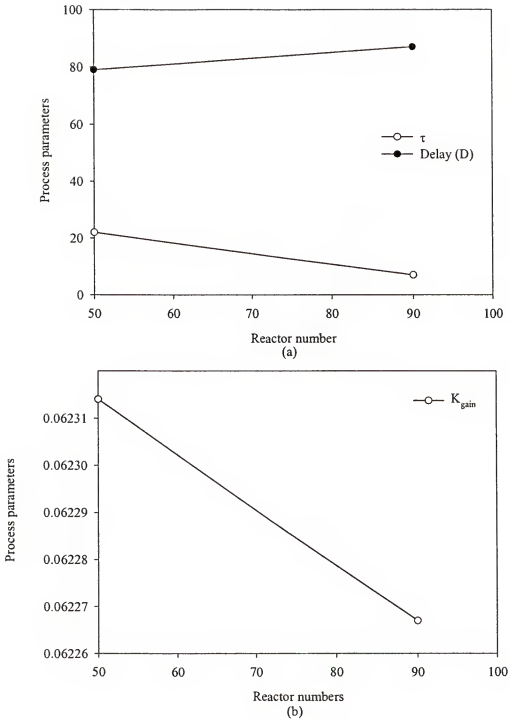

Figure 4-19. Process parameters obtained from open loop program ($\Delta t = 20$ sec)

4.5 Closed-Loop Simulation Study

The tuning of the master closed controller is performed using the apparent process parameters discussed in the previous section. The daily change in flow rate of wastewater is assumed to be sinusoidal, as shown in Figure 4.19.

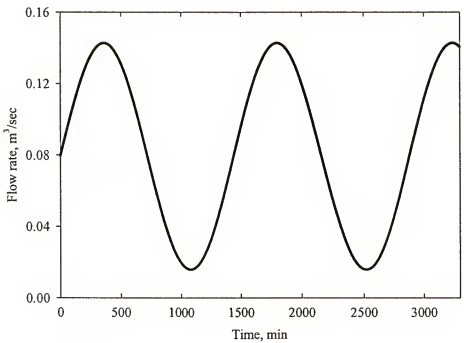

Figure 4-20. Variation of flow rate with time

PID form of the master controller was used along with dead time compensation for the tuning process. One fixed tuning was evaluated for different time increments and number of reactors, and the corresponding apparent process parameters. The master PID controller was tuned by trial and error, and was fixed to the following constant settings

$K_c = 0.5$

$\tau_I = 100$ m

$\tau_D = 0$

It is shown in Figure 4.21 that when the time increment is 0.5 sec, the closed loop performance is poor. Good performance is obtained when the final probe measured value is equal to the set point of 2.8 mg/L. Hence, the deviation-variable form of the final probe measurement must be zero in Figure Figure 4-20 for perfect control. Clearly, the final-probe value is not close to zero, indicating poor performance. The time increment was changed to 5 sec, and the closed loop program was run again with the same controller settings. The resulting response is shown in Figure 4-22, where the performance is improved because the deviation values of the final probe measurements are close to zero. Repeating this procedure for integration step sizes of 10 sec and 20 sec leads respectively to Figures 4.23 and 4.24, where improved control is attained.

In summary, if the process model used in the Smith Predictor block is adequately described by discrete models with increments ranging from 5 sec to 20 sec, the proposed control strategy delivers good performance. Further studies are needed to determine the relationship between the control scheme and the appropriate step size selection for increment values less than or equal to $\Delta t = 0.5$.

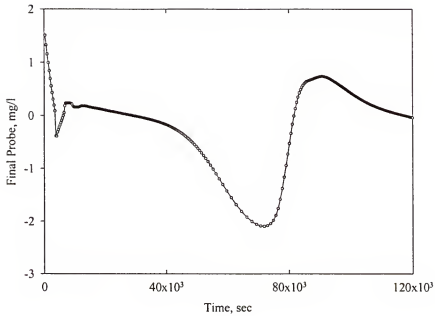

Figure 4-21. Simulation results (K_{gain} = 0.06155, Reactor num. = 500, τ = 10, Δt = 0.5 sec, D = 85)

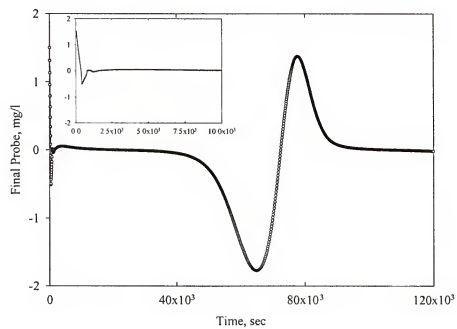

Figure 4-22. Simulation results (K_{gain} = 0.06215, Reactor num. = 200, τ = 10, Δt = 5 sec, D = 85)

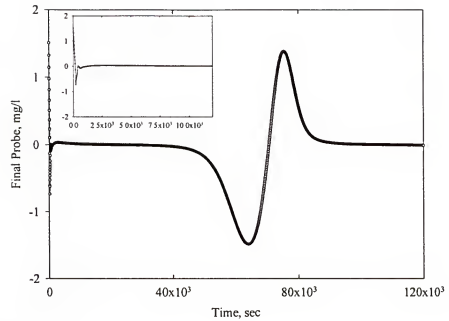

Figure 4-23. Simulation results (K_{gain} = 0.06225, Reactor num. = 100, τ = 16, Δt = 10 sec, D = 81)

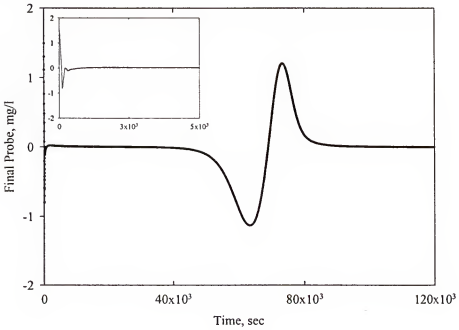

Figure 4-24. Simulation results (K_{gain} = 0.06231, Reactor num. = 50, τ = 22, Δt = 20 sec, D = 79)

4.6 Conclusion

A cascade control with dead-time compensation strategy was applied along with an odometric transformation to evaluate the closed loop performance of a process for wastewater treatment with chlorine. The odometric transformation permits designing a Smith Predictor with a constant dead time. An open loop simulation program was used to calculate the maximum number of reactors required to approximate the plug flow reactor, and the corresponding apparent process parameters were determined. These process parameters were used in the closed loop program to obtain a stable response for the system. The delay was calculated from the open loop response, and it was found to be very close to the delay that was calculated theoretically using the odometric transformation. The simulation study suggests that a time increment of 20 sec is adequate for carrying out a discrete approximation to the continuos system. The results show that the joint application of the method of characteristics and the odometric transformation may lead to successful control performance for the chlorine disinfection of wastewater.

CHAPTER 5
DISSOLUTION CAPACITY OF METAL IONS FROM CRUDE KAOLIN PARTICLES IN THE ABSENCE AND THE PRESENCE OF ANIONIC DISPERSING AGENTS

5.1 Introduction

In this study, the reaction mechanism between the dispersing agents and kaolin particles were studied and the dissolution capacity of metal ions (Al^{+3}, Si^{+4}) were identified from kaolin particles in the absence and presence of dispersing agents. We believed that there was a relationship between the rheological behavior and the soluble salt concentration in the dispersion. Three anionic dispersing agents, sodium polyacrylate (NaPAA), sodium hexametaphosphate (NaHMP) and sodium silicate (Na-Silicate) were used based on their effect on producing a stable dispersion for this purpose. The effect of pH was also studied to identify weather it had effect on solubility of metal ions.

We also have conducted statistically designed experiments to study the solubility of metal ions from kaolin particles in the presence of different dispersing agents used to prepare highly concentrated kaolin slurries and also as a function of the suspension pH. Central Composite Design method (CCD) was used to identify whether there is any difference on the dissolution capacity of metal ions using NaOH and Na_2CO_3 as pH modifiers. Using Box Behnken method completed the rest of the research. Control variables were the dosage of the dispersing agents, solids concentration, time, and the pH of the dispersion.

5.2 Materials and Methods

5.2.1 Materials

The Engelhard Corporation supplied the kaolin particles, which was used in this study. Its surface area was determined as 20.32 $m^2.g^{-1}$ by the BET (Brunauer-Emmett-Teller) method, using nitrogen adsorption isotherm (Quantachrome NOVA 1200). SEM picture is shown in Figure 5-1. The particle size distribution was determined by COULTRE LS 230, using light scattering technique, and d_{10}, d_{50}, d_{90} found as 0.301, 3.363 and 13.37 μm respectively. The density of the powder was measured to be equal to 2.72 $g.cm^{-3}$, using Helium Ultrapycnometer.

Three anionic dispersing agents used in this study were NaPAA (43.1% solids (wt)) of molecular weight 3,400 $g.mol^{-1}$ with a polydispersity index of 1.2, NaHMP (30% solids (wt)) and Na-Silicate (37.5% solids (wt)).

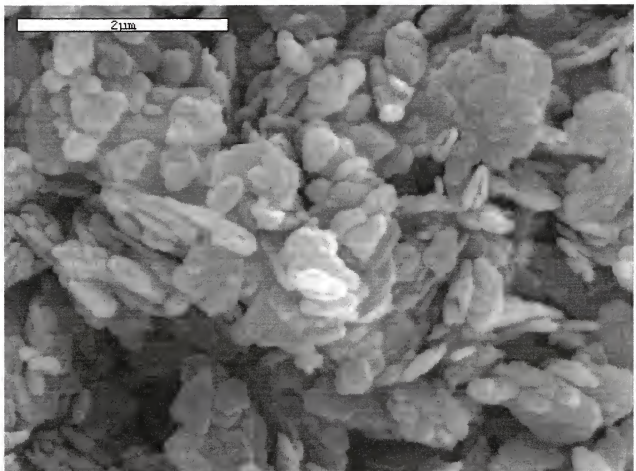

Figure 5-1. Kaolin particles

5.2.2 Sample Preparation

All kaolin dispersions used in this study were prepared using the following procedure:

15 g/L stock solution was prepared for each dispersing agents. A certain amount of water, which was produced by a Millipore filtration system, including less than 7 ppb carbon and its internal specific resistance was 18.2 M , and dispersing agent were initially added into the centrifuge tube. Then, kaolin particles were slowly added with continuos stirring and pH was adjusted. After preparing the suspensions, they were left on Burrell Model 75 wrist action shaker for different times. They were centrifuged at 15,000 rpm for 15 min using Beckman Model J2-21 Centrifuge. Supernatant was removed genteelly and poured into a small glass test tube. All samples were kept in the cooler for at least one day to have all clay particles settle down and the clear supernatant was analyzed for aluminum and silicon using a Perkin Elmer Plasma (ICP-AES). The metal ion concentrations are reported as mg/L in the supernatant.

5.2.3 Chemical Analysis

A certain amount of kaolin powder was dried at 100-110°C to remove moisture at least one hour before analysis. It was cooled until room temperature and 0.5 g was taken to analyze. Half of 5 g Na_2CO_3 was added and mixed with kaolin and then rest of them was added and mixed. In order to decompose the structure of kaolin, it was kept 30 min in the preheated furnace at 900°C. After the sample was cooled, it was put into 50 ml 1/1 HCl (vol.) solution in the glass beaker. Expected chemical reaction was observed and only platinum crucible was removed from medium after washing with distilled water very well in the beaker. The solution, which was in the beaker, was boiled until all water was

evaporated. After evaporation, 50 ml HCl was added. This solution was filtered using ashless filter paper (Watman number 40). Beaker was washed many times with distilled water and solution filtered. Filter paper was washed until filtered solution became colorless. An empty clean porcelain crucible was weighed and filter paper with content was placed in it. They were kept in the preheated furnace one hour at 900°C and then cooled to room temperature. Filtered solution was completed to 1000 ml and a certain amount of solution was used for chemical analysis at the ICP-AES. Elemental analysis is shown in Table 5-1

Table 5-1. Chemical composition of Georgia Crude Kaolin

Assay	%	Element	mg/L
Al_2O_3	38.04	Al^{3+}	198.2
SiO_2	46.44	Si^{4+}	216.9
TiO_2	1.19	Ti^{4+}	0.166
Fe_2O_3	0.18	Fe^{3+}	0.0258
L.O.I.	14.4	---	---
CaO	0	Ca^{2+}	0
MgO	0	Mg^{2+}	0
Total	100.25		415.29

5.3. Dissolution Capacity of Metal Ions

5.3.1 Effect of Solids Concentration in the Absence of Dispersing Agents

Dissolution of metal ions from kaolin particles was investigated in the absence of dispersing agent at various solid concentrations. Experimental results showed that released silicon ions were increased with increasing solid concentration. However, aluminum ions were not observed in the suspension with increasing solid concentration. The solubility of $Al(OH)_3$ in water is very low in the pH range of 4 - 10 (Wefers and Misra, 1987; Mcmurry and Fay, 1998). Released aluminum ions probably precipitated as aluminum hydroxide. This is shown in Figure 5-2

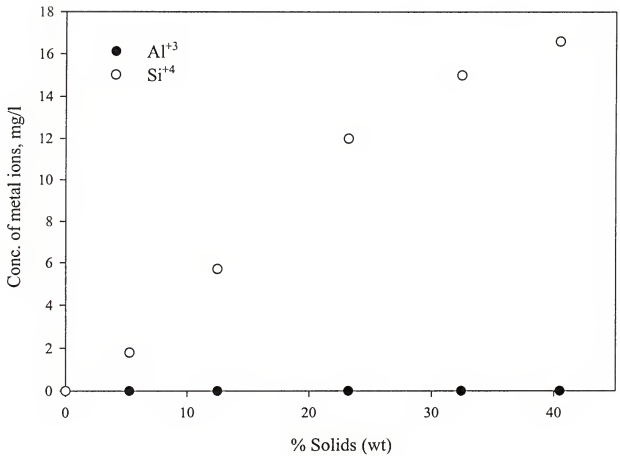

Figure 5-2. Concentration of aluminum and silicon ions from kaolin particles in the absence of dispersing agents

5.3.2 Effect of the Dosage of Dispersant without pH Adjustment

Three different dispersing agents have very significant affect on the dissolution capacity of metal ions from kaolin particles. Figures 5-3 and 5-4 show that the released aluminum and silicon ions are increasing with increasing the dosage of any dispersing agents.

In Figure 5-3, it is shown that NaHMP produced highest amount of aluminum in the suspensions. The reaction between kaolin and NaHMP leads to increase the amount of released aluminum ions, since phosphorous ions have strong affinity to aluminum ions. Released aluminum ions appear in the solution as a complex with phosphate (Yuan et al. 1998). The phosphorous ions $(PO_3)^{-3}$ will compete with OH^- for aluminum and reacts with $(-OH_2^+)$ surface groups of aluminum to form complex ions. These released aluminum ions remain in the solution as water-soluble form. Yuan et al. (1998), who had studied the influence of dispersing agents, observed similar behavior on solubility of calcined kaolin.

When NaPAA was used and the dosage was increased, a large amount of aluminum was released until the dosage 5 mg/(g solids) and then it was increased slowly at the high dosage. In Figure 5-3, it is shown that NaPAA and NaHMP have similar reaction mechanisms with kaolin particles. The explanation of high soluble aluminum ions is the reaction between kaolin particles and polymer, which produces aluminum-polymer complex ions, and these complex ions stay in the suspension in water-soluble form or without precipitating (Yuan et al. 1998). The pH increment was just due to negatively charged polymer and it was increasing from 5.26 to 6.57. It is shown in Figure 5-5. PAA strongly adsorbs on alumina side of kaolin. Electrostatic and hydrogen

bonding are important at the adsorption mechanism. When the pH of the solution increases, the number of hydrogen donor groups ($-OH_2^+$), which is provided for the hydrogen bonding, decreases and forms ($-O^-$) surface groups. As a result of this, adsorbed amount of polymer decreases due to the repulsion of two negatively sides (Subramanian et al 1995). There are electrostatic attraction between ($-OH_2^+$) surface groups and the ($-COO^-$) functional group of polymer. This attraction forms the complex ions. When the pH is below pzc, adsorption of polymer occurs between ($-OH_2^+$) surface group of aluminum and the ($-COO^-$) functional group of polymer. This adsorption produces water-soluble complex ions.

Na-silicate produced the lowest amount of aluminum ions. Its effect on pH increment was greater than the other two dispersing agents have. The explanation of these less amount of dissolved aluminum ions may be due to high pH increment. When sodium silicate is used, the pH of the solution is increased and it affects the ($-OH_2^+$) surface groups of alumina site. This hydrogen donor group ($-OH_2^+$) becomes ($-O^-$). Since experimental conditions are still under the pzc for alumina site, there is still positively charged alumina sites. Adsorption takes place between negatively charged silicate ions (SiO_4^{-4}) and the ($-OH_2^+$) surface groups of alumina site.

The same result was also observed for silicon ions and it is shown in Figure 5-4. NaPAA and NaHMP have almost the same affect on the dissolution capacity of silicon. Since Na-Silicate includes large amount of silicon itself, it appeared highest amount in the suspension.

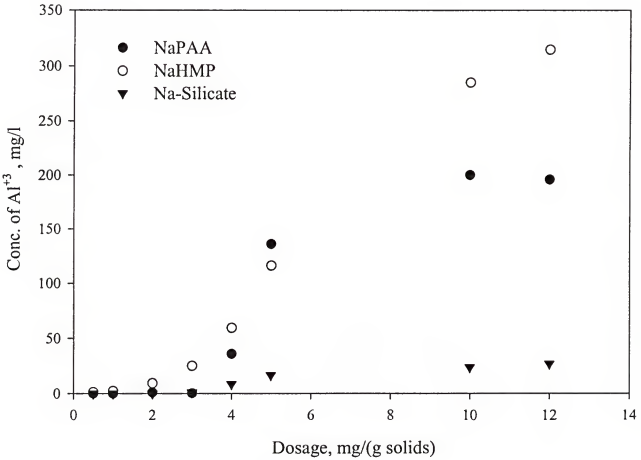

Figure 5-3. Concentration of Al^{3+} as a function of dispersants dosage in the supernatant at fixed level of 55% solids (wt)

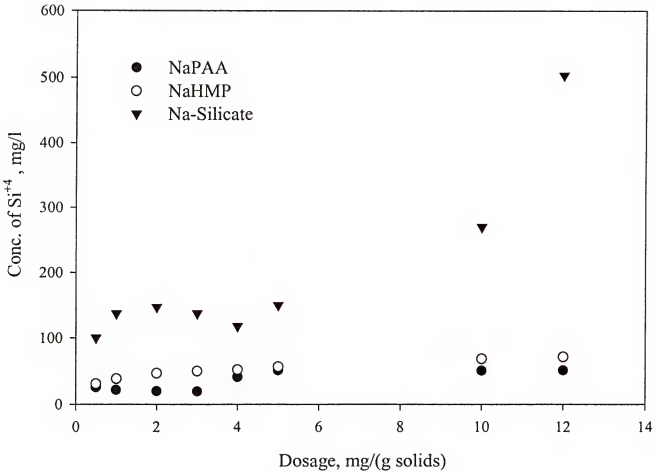

Figure 5-4. Concentration of Si^{4+} as a function of the dispersants dosage in the supernatant at fixed level of 55% solids (wt)

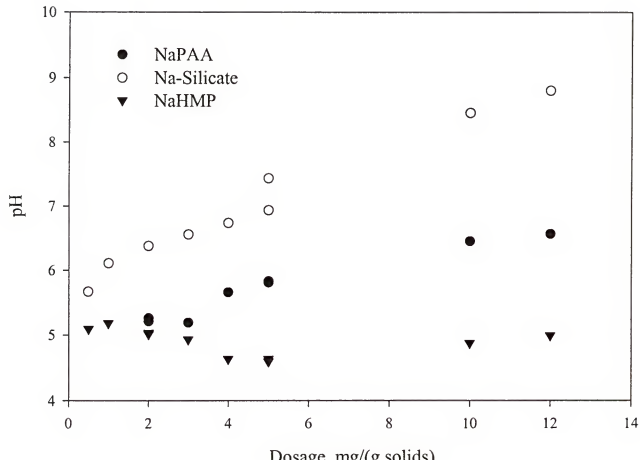

Figure 5-5. Variation of pH in the dispersions at the various dosage of dispersants at fixed level of 55% solids (wt)

5.3.3 Effect of %Solid (WT) in the Presence of Dispersants without pH Adjustment

Figures 5-6 and 5-7 show the solid loading dependency of released aluminum and silicon ions at fixed level of 5 mg/(g solids) dosage for NaPAA, NaHMP and Na-Silicate. It is shown that addition of more kaolin particles at a fixed dosage produces large amount of soluble aluminum and silicon ions for NaPAA and NaHMP. There is almost a linear correlation between them. The larger the kaolin powder, the highest the available aluminum and silicon ions from the kaolin particles. The suspension was not well dispersed at high solid loading, due to fact that dispersing agents were not enough to react with all aluminum of kaolin to produce complex ions and to complete adsorption. Since Na-Silicate had already a large amount of silicon, it appeared in the suspension with its own silicon and released silicon. But at high solid loading, since the suspension was not well dispersed or Na-Silicate was not enough to dissolve silicon, concentration of silicon was not increased. In addition, when the solid concentration was more than 60% solids (wt), it started to decrease.

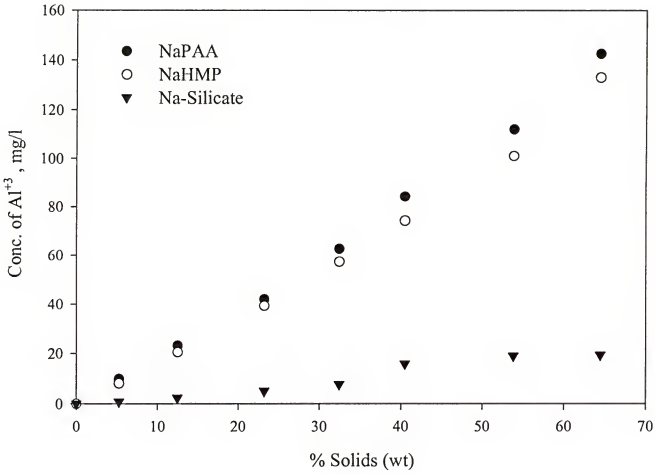

Figure 5-6. Concentration of Al^{3+} as a function of %solids (wt) in the supernatant using three dispersing agents a dosage level of 5

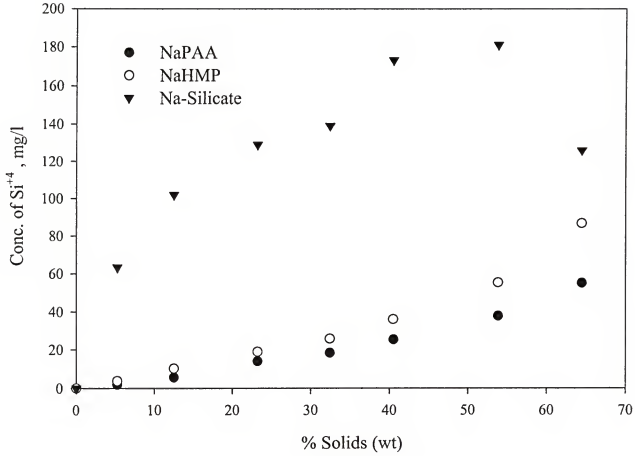

Figure 5-7. Concentration of Si^{4+} as a function of %solids (wt) in the supernatant using three dispersing agents a dosage level of 5

5.3.5 Effect of pH

Solubility of aluminum strongly depends on the pH of the dispersion and it is in the form of $Al(OH)_3$ precipitation in the pH range of 4 and 10 (Devidal et al. 1997). Solubility of silicon also depends on the pH of the dispersion and it is in the form of SO_2 below the pH 10 at room temperature (Okamoto, 1957). In Figure 5-2, it shown that silicon ions are only the released ions from kaolin particles in the absence of dispersing agent. Released aluminum ions probably precipitated as aluminum hydroxide. In Figure 5-8, it is shown that the pH increment is decreasing the concentration of silicon in the dispersion.

Since, in the range of pH 4-10, the solubility of $Al(OH)_3$ is very small; addition of OH^- ions precipitates aluminum ions. The same reaction takes place by the addition of H_3O^+ ions. Because aluminum is an amphoteric material and it gives the following reaction in the range of pH 4-10 (Mcmurry and Fay, 1998)

$$Al(OH)^-_4(aq) + H_3O^+ \leftrightarrow Al(OH)_3(s) + 2H_2O \quad (5.1)$$

$$Al^{3+}(aq) + 3OH^- \leftrightarrow Al(OH)_3(s) \quad (5.2)$$

and its reaction in acid and base are

$$Al(OH)_3(s) + 3H_3O^+ \leftrightarrow Al^{3+}(aq) + 6H_2O \quad (5.3)$$

$$Al(OH)_3(s) + OH^- \leftrightarrow Al(OH)^-_4(aq) \quad (5.4)$$

Based on these reactions, it is shown that concentration of aluminum is decreasing by increasing and decreasing pH.

Okamoto et al. (1957), Iler (1973) and Yuan et al. (1998) explain these decreasing of silicon concentration with the formation of an aluminosilicate surface (alumino-silicate gel) on the kaolin particles. When aluminum ions are released from particle, it starts to

reduce the dissolution of silicon ions from particles. Because the dissolved aluminum ions are adsorbed on the silica and they produced an aluminosilicate surface on the kaolin particles. This aluminosilicate surface or alumino-slicate gel is pH dependent and its reaction mechanism is given as

$$\begin{array}{c} | \\ --\mathrm{Si(OH)} \\ | \end{array} + [\mathrm{Al(H_2O)_3}]^{3+} \leftrightarrow \begin{array}{c} | \\ --\mathrm{Si\,O[Al(H_2O)_3]^{2+}} \\ | \end{array} + \mathrm{H^+} \qquad (5.5)$$

In this reaction mechanism, it is clearly shown that increases in pH decreases hydrogen ions and due to the fact that the reaction tends to go to the new equilibrium conditions and more aminosilicate surface occurs and this layers prohibits the release of silicon ions from kaolin particles. All these results are in agreement with the work of Okamoto et al. (1957), Iler (1973) and Yuan et al. (1998).

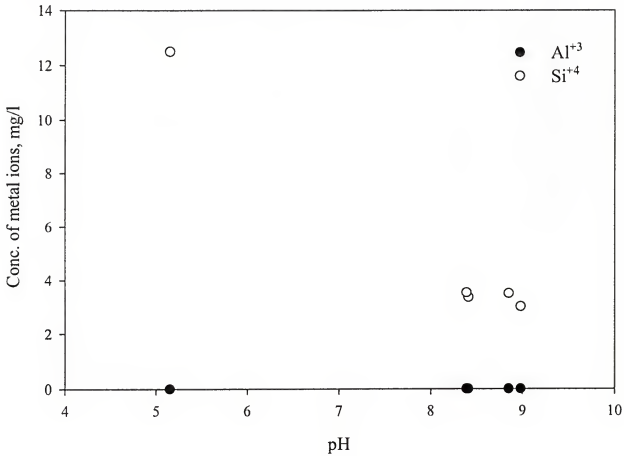

Figure 5-8. Concentration of metal ions as a function of pH from kaolin at fixed level of solid concentration (35% solids (wt)) in the absence of dispersant

5.4 Dissolution Capacity of Metal Ions using Design of Experiment (DOE) Software

5.4.1 Effect of pH Modifiers on Solubility of Metal Ions

Since in practice, Na_2CO_3 is used as pH modifier which may have a different effect on solubility of metal ions from kaolin particles than NaOH, in this part of work statistically designed experiments based on Central Composite Design (CCD) were conducted to investigate the effects of Na_2CO_3 and NaOH on solubility of metal ions an also, to examine the similarity of the effects of these two pH modifiers on solubility of metal ions from kaolin particles. Experimental conditions along with the solubility of metal ions are summarized in Table 5-2.

Two-sample t-Test is a statistical analysis method that can be used to identify if there is any difference between two independent samples that were observed. Sample sizes are usually less than 30 for this test (Mann, 1995). Otherwise, z-Test is more appropriate for the analysis. In this part of the research, since the sample size was 24 for each set of experiment, t-Test was performed and results were compared with t-Test values that were obtained from the table. In the Two-Sample t-Test, the hypothesis was the means of the two samples were different and the population means were unknown but equal. Under these conditions, the test was performed for dissolved aluminum and silicon ion concentrations at the 95% confidence interval. The calculated values of t for the samples were 0.0566 for aluminum and –0.1869 for silicon ions (McClave et al. 1997). Comparison of these values with the standard values of t (± 2.02 over 95% confidence interval) given from the table show that the values of the test statistic t = 0.0566 for aluminum and t = -0.1869 for silicon are in the nonrejection region, and

consequently it is concluded that there is not any difference in the solubility of metal ions from kaolin using NaOH or Na_2CO_3 as pH modifiers.

Table 5-2. Dissolved aluminum and silicon ion concentrations from Georgia Crude kaolin under various experimental conditions in the presence of NaPAA using NaOH and Na_2CO_3 as pH modifiers

% Solids (wt)	Time, hr	Dosage, mg/(g solids)	pH		Conc. of Al^{+3}, mg/l		Conc. of Si^{+4}, mg/l	
			NaOH	Na_2CO_3	NaOH	Na_2CO_3	NaOH	Na_2CO_3
35	18	5	6.76	6.81	50.50	54.00	12.00	14.10
35	18	5	6.85	6.27	49.50	59.90	11.60	15.00
10	12	0	7.33	6.07	0.00	0.00	0.955	1.65
10	12	0	7.50	7.79	0.00	0.00	1.10	2.15
10	24	0	7.26	6.14	0.00	0.00	3.52	2.23
10	24	0	7.80	8.13	0.00	0.98	1.33	1.94
10	12	10	7.13	7.18	17.40	20.00	5.26	5.36
60	12	10	6.33	6.33	210.00	215.00	36.30	29.20
10	12	10	7.88	7.84	9.63	7.09	5.57	4.31
60	12	10	7.74	7.72	30.70	29.70	29.50	26.00
10	24	10	7.19	7.00	18.80	20.30	6.65	6.52
60	24	10	6.31	6.27	207.00	213.00	38.60	35.20
10	24	10	7.53	7.67	9.24	8.93	4.85	4.82
60	24	10	7.29	7.65	40.00	31.00	27.80	25.30
35	18	5	6.08	5.91	65.90	67.90	14.50	16.90
35	18	5	6.02	5.91	66.70	69.40	13.60	16.20
35	18	5	8.03	8.74	7.74	13.00	9.75	14.30
35	18	5	8.72	8.69	13.50	11.00	15.30	12.50
35	6	5	6.88	6.73	53.90	55.00	12.30	9.02
35	6	5	6.74	6.83	59.40	54.80	14.50	9.98
35	30	5	6.77	7.03	37.90	37.20	18.70	16.70
35	30	5	6.84	6.85	53.70	51.20	18.10	18.20
35	18	15	6.88	6.88	74.60	71.30	16.60	14.00
35	18	15	6.88	6.90	65.20	75.10	11.50	16.20

5.4.2 Effect of Dispersing Agents on Solubility of Aluminum Ions

In this part of research, Box Behnken method was used to design the experimental conditions and investigate the effect of factors on the dissolution capacity of metal ions. Since, in Central Composite Design, the extremes of the design may fall outside of the domain of independent variables, which sometimes make it very difficult or impossible to prepare the sample, Box Behnken method was employed for the design of experiments. Since, using this method, all conditions will be within the domain of the design, it is more appropriate than CCD. Experimental conditions are summarized in Table 5-3.

Both the dosage of NaPAA and the pH of the suspension as shown in Figure 5-9 affect solubility of aluminum ions from kaolin. It is a 3-D plot for the concentration of aluminum ions in the supernatant as a function of pH of the suspension and the dosage of NaPAA as the dispersing agent. It can be observed from Figure 5-10, which represents the contours for the effects of pH and Na-PAA dosage on the concentration of aluminum ions in supernatant. The dissolved aluminum ion concentration increases from nearly 20 mg/l to 110 mg/L when the dosage of NaPAA in the dispersion changes from 3 mg/(g solids) to 7 mg/(g solids). PAA strongly adsorbs on alumina side of kaolin. Adsorption mechanism was explained in Section 5.3.2

The solubility of $Al(OH)_3$ in water is very low in the pH range of 4 - 10 (Wefers and Misra, 1987; Mcmurry and Fay, 1998, Holtzclaw et al 1991). At low dosage, the amount of aluminum concentration is decreasing with increasing pH but the effect of pH is not clearly seen since there is no significant amount of dissolved aluminum ions in the dispersion. However, at high dosage, since there is considerably large amount of aluminum, addition of an appropriate amount of OH^- ions into the dispersion decreases

the concentration of aluminum ions and forms $Al(OH)_3$ precipitation and alumino-silicate gel. This precipitation is water-insoluble in the pH range of 4 - 10. These results are shown in Figure 5-11.

Figure 5-12 is the surface response plot for the effects of suspension's pH and NaHMP dosage (at fixed levels of time and solid content) on solubility of aluminum from kaolin particles. Figure 5-13 represents the contour plots for aluminum ion concentration as a function of the suspension pH and dosage of NaHMP.

The other common dispersant used in kaolin industry is sodium silicate. Its effect on pH increment was greater than the other two dispersing agents have. Therefore, it produced less amount aluminum complex in the dispersion. Figures 5-14 and 5-15 show the effect of Na-Silicate dosage and pH on solubility of aluminum in the dispersion.

Table 5-3. Factors and levels for experimental design using Box Behnken method

Factor	Name	Units	Low Actual	High Actual	Low Coded	High Coded
A	% Solids (wt)		10	60	-1	1
B	pH		6	8	-1	1
C	Time	hr	2	24	-1	1
D	Dosage	mg/(g solids)	3	7	-1	1

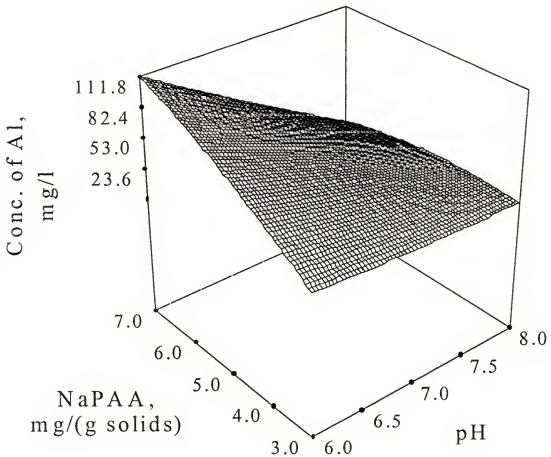

Figure 5-9. Surface response plot for the effects of pH and NaPAA dosage on solubility of aluminum from kaolin (time = 13 hrs, %solids (wt) = 35)

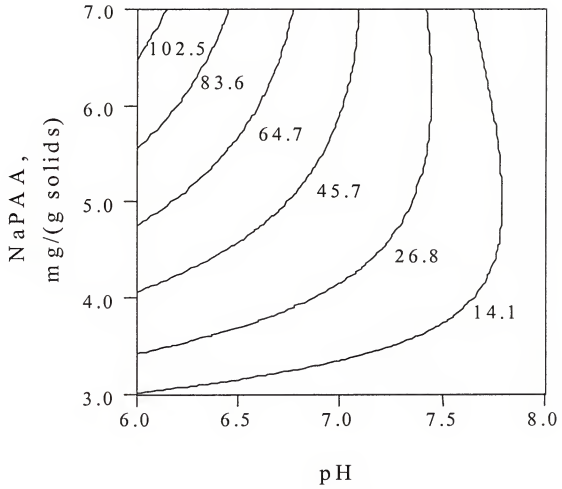

Figure 5-10. Contour plots for the effects of pH and NaPAA dosage on solubility of aluminum from kaolin (time = 13 hrs, %solids (wt) = 35)

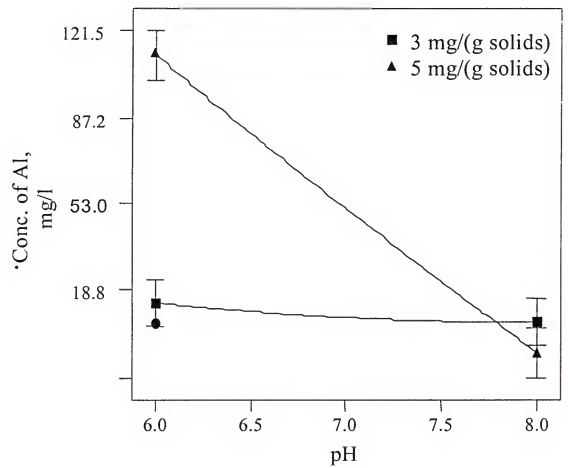

Figure 5-11. Interaction graph for the effects of NaPAA and pH on solubility of aluminum from kaolin (time = 13 hrs, %solids (wt) = 35)

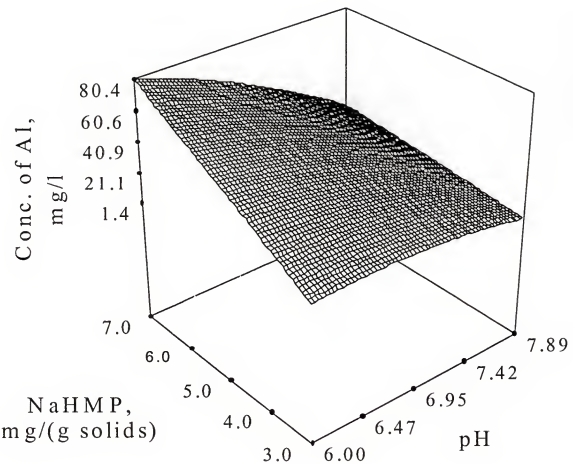

Figure 5-12. Surface response plot for the effects of pH and NaHMP dosage on solubility of aluminum from kaolin (time = 13 hrs, %solids (wt) = 35)

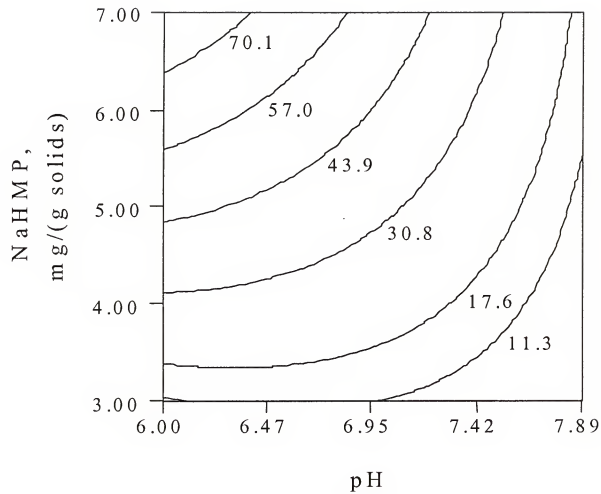

Figure 5-13. Contour plots for the effects of pH and NaHMP dosage on solubility of aluminum from kaolin (time = 13 hrs, %solids (wt) =35)

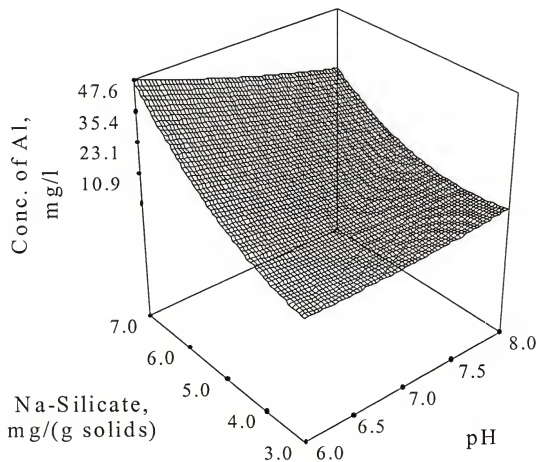

Figure 5-14. Surface response plot for the effects of pH and Na-Silicate dosage on solubility of aluminum from kaolin (time = 13 hrs, %solids (wt) = 35)

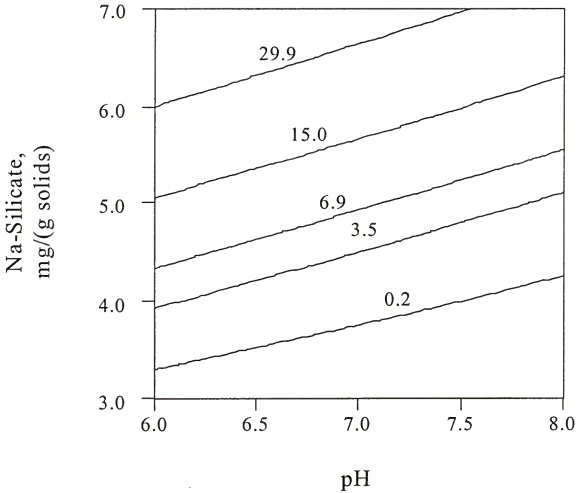

Figure 5-15. Contour plots for the effects of pH and Na-Silicate dosage on solubility of aluminum from kaolin (time = 13 hrs, %solids (wt))

5.4.3 Effect of Dispersing Agents on Solubility of Silicon Ions

Dissolution capacity of silicon ions was also investigated under the same experiment conditions as a function of pH, time, solid concentration and the dosage of the dispersant in the suspension.

Solubility of silica is pH dependent (Okamoto et al. 1957). Figures 5-16 and 5-17 show that the concentration of silicon ions is decreasing and then it starts to increase again after a certain pH. It is well known that NaPAA produces soluble aluminum complex ions and this aluminum reduces the solubility of silica. Concentration of aluminum increases with increasing the dosage of NaPAA and aluminum ions form more alumino-silicate gel and reduce the solubility of silicon ions. After the formation of alumino-silicate gel reaches to the equilibrium condition, the pH of the suspension becomes effective and starts to increase the concentration of silicon ions. Okomato (1957) showed that the solubility of silica is slightly increasing in the range of pH 6 and 8 and this work is in agreement with his work.

Silicon concentration usually increased with increasing dosage of NaHMP, but decreased with increasing the pH of the suspension. This situation was explained with the formation of aluminosilicate surface or alumino-slicate gel on the kaolin surface (Yuan et al. 1998). It is shown in Figures 5-18 and 5-19.

When sodium silicate was used, the soluble silicate ions appeared at the highest amount because of its own silicon contribution. The pH of the suspension significantly affected its dissolution and increase in the pH increased the formation of aluminosilicate surface on the particles. Therefore, a big decrease was observed at the concentration of silicon. These results are shown in Figures 5-20 and 5-21.

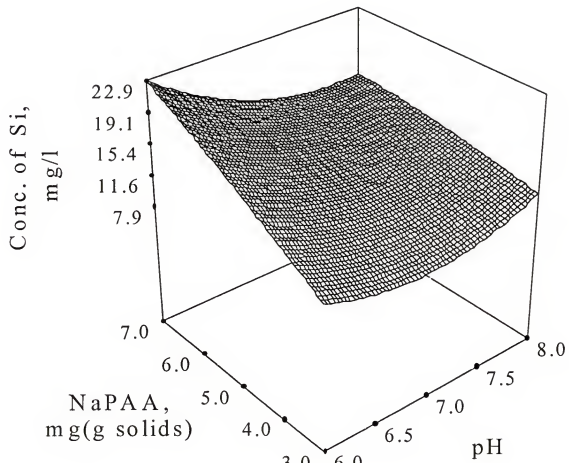

Figure 5-16. Surface response plot for the effects of pH and NaPAA dosage on solubility of silicon from kaolin (time = 13 hrs, %solids (wt) = 35)

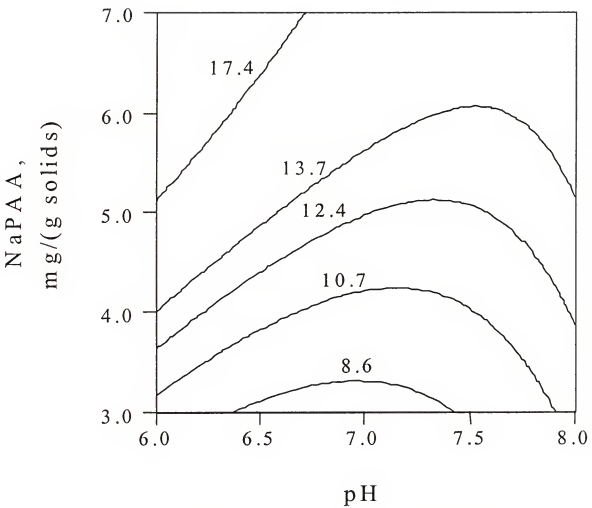

Figure 5-17. Contour plots for the effects of pH and NaPAA dosage on solubility of silicon from kaolin (time = 13 hrs, %solids (wt)= 35)

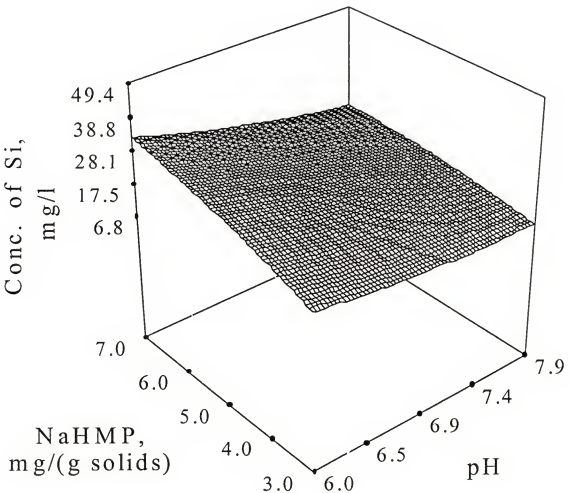

Figure 5-18. Surface response plot for the effects of pH and NaHMP dosage on solubility of silicon from kaolin (time = 13 hrs, %solids (wt) = 35)

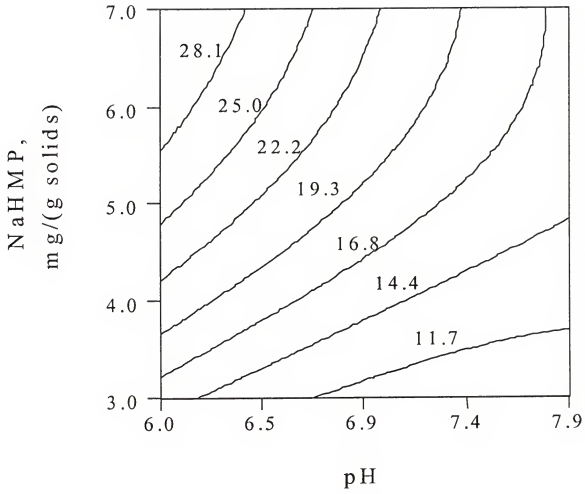

Figure 5-19. Contour plots for the effects of pH and NaHMP dosage on solubility of silicon from kaolin (time = 13 hrs, %solids (wt)= 35)

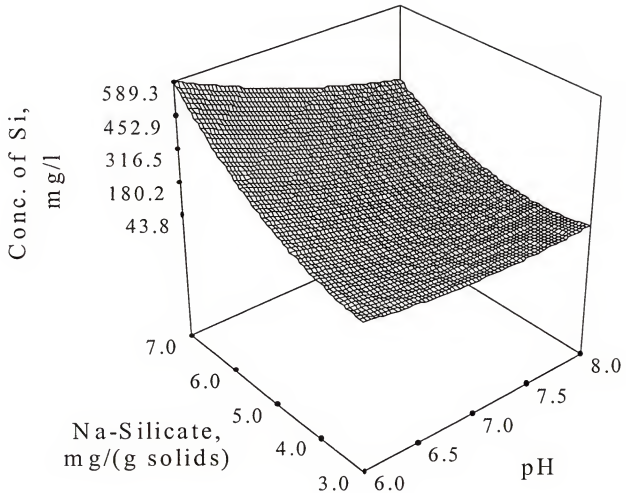

Figure 5-20. Surface response plot for the effects of pH and Na-Silicate dosage on solubility of silicon from kaolin (time = 13 hrs, %solids (wt) = 35)

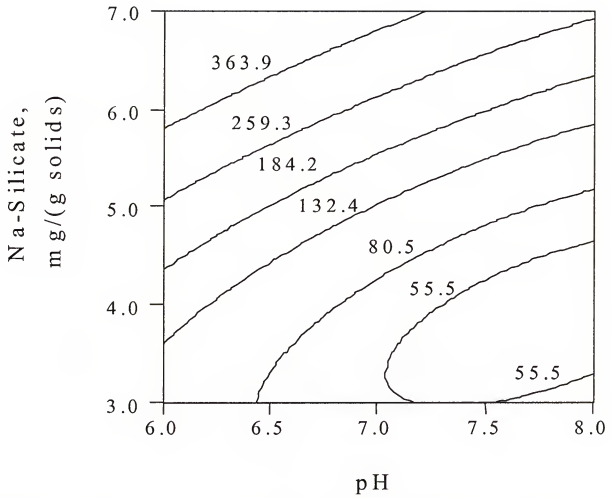

Figure 5-21. Contour plots for the effects of pH and Na-Silicate dosage on solubility of silicon from kaolin (time = 13 hrs, %solids (wt) = 35)

5.5 Predictive Models for the Concentration of Aluminum and Silicon Ions in the Presence of Dispersing Agents

Dissolution capacity of aluminum and silicon ions from kaolin particles was investigated as a function of pH, time, solid concentration and the dosage of the dispersants. Model parameters for the full and the best linear regression models based on f-Test values are given in Tables 5-4 and 5-5.

A linear regression model that consists of the main variables, second and higher order interactions can be expressed as

$$Y = \alpha_o + \sum_{i=1}^{4} \alpha_i X_i + \sum_{i=1}^{4} \sum_{i<j}^{4} \alpha_{ij} X_i X_j + \sum_{i=1}^{4} \alpha_{ii} X_i^2 \qquad (5.6)$$

where Y is the estimate of the response variable, and X_1 (%solids (wt)), X_2 (pH), X_3 (Time), and X_4 (Dosage) are the independent variables. Regression parameters are given as α_o, α_{ij}, and α_{ii} (Ott, 1988).

Analysis of the data based on the full regression model indicates that almost all factors affect the dissolved aluminum and silicon ion concentrations. Some factors or interactions are more significant and therefore, insignificant terms can be eliminated without losing the originality of the model or without changing the R-squared value significantly. This elimination can be done based on the test statistic F values, which were already provided by the software. The test statistic F indicates the significance of the independent variables in the model and if the test statistic value is less than 0.1, they can be eliminated. The result of elimination provides the best model for the system and since it includes less independent variables and regression parameters, it needs less number of experiments to identify the model. The best models for the dissolved

aluminum and silicon from kaolin in the presence of different dispersants are summarized in Table 5-5.

The diagnostic results provide different plots that can be used to analyze the results. In Figure 5-22, residual values are spread across all levels of the predicted values and they are independent of their predicted values. These results indicate that experiments were conducted well and any of result is not carrying any significant error. In Figure 5-23, the predicted values and observed values are in a very good agreement and they almost remain on the same straight line. Therefore, the model, which was provided by the software, represents the system well.

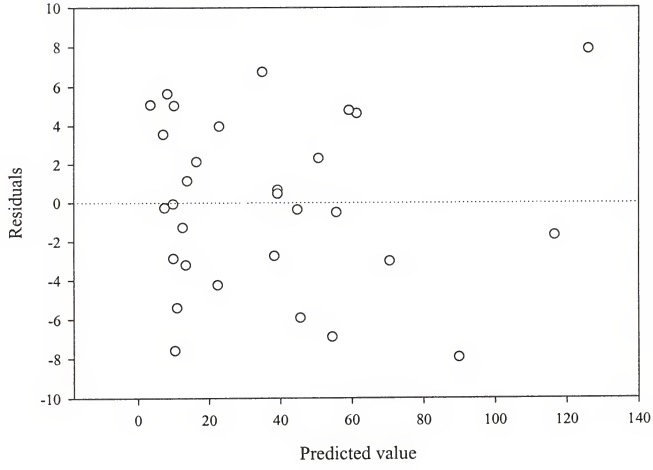

Figure 5-22. Residuals versus predicted values for the effect of NaPAA dosage on solubility of aluminum from kaolin particles

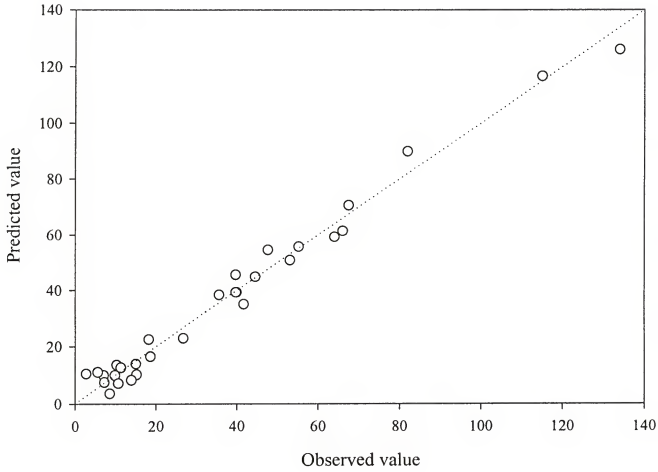

Figure 5-23. Predicted versus observed values for the effect of NaPAA dosage on solubility of aluminum from kaolin particles

Table 5-4. Complete and the best linear regression models for the dissolution of aluminum ions from kaolin in the presence of different dispersing agents

VARIABLES	REGRESSION PARAMETERS			VARIABLES	REGRESSION PARAMETERS		
	NaPAA	NaHMP	Na-Silicate		NaPAA	NaHMP	Na-Silicate
a_o	- 400.265	- 577.792	21.472	a_o	- 521.140	- 560.621	- 14.775
% Solid	4.949	3.854	- 1.419	% Solid	5.416	3.749	0.035
pH	39.551	126.306	- 3.053	PH	71.250	124.111	-
Time	- 0.253	0.220	0.538	Time	-	-	- 0.529
Dosage	111.986	52.417	3.932	Dosage	112.306	50.075	3.801
% Solid^2	$4.052 * 10^{-3}$	- 0.001	0.003	% Solid^2	-	-	-
pH^2	2.075	- 6.111	1.042	pH^2	-	- 5.957	-
Time^2	$4.977 * 10^{-3}$	0.006	0.016	Time^2	-	-	-
Dosage^2	- 2.042	- 0.298	2.692	Dosage^2	- 2.149	-	-
% Solid * pH	- 0.918	- 0.683	0.141	% Solid * pH	- 0.959	- 0.676	-
% Solid * Time	$- 9.648 * 10^{-3}$	- 0.002	0.018	% Solid * Time	-	-	0.021
% Solid * Dosage	0.465	0.356	0.034	% Solid * Dosage	0.462	0.355	-
pH * Time	0.087	- 0.024	- 0.316	pH * Time	-	-	-
pH * Dosage	- 13.768	- 7.375	- 3.607	pH * Dosage	- 13.749	- 7.496	-
Time * Dosage	- 0.053	- 0.016	0.188	Time * Dosage	-	-	-
R	0.9814	0.9946	0.9693	R	0.9779	0.9932	0.8637
Adj.R^2	0.9615	0.9888	0.9335	Adj.R^2	0.9701	0.9908	0.8389

Table 5-5. Complete and the best linear regression models for the dissolution of silicon ions from kaolin in the presence of different dispersing agents

VARIABLES	REGRESSION PARAMETERS			VARIABLES	REGRESSION PARAMETERS		
	NaPAA	NaHMP	Na-Silicate		NaPAA	NaHMP	Na-Silicate
a_0	106.793	21.407	1487.660	a_0	13.698	- 18.034	687.453
% Solid	- 0.291	1.218	-16.285	% Solid	- 0.578	1.518	- 13.288
pH	- 32.856	-15.824	-377.572	pH	-	4.193	- 55.953
Time	0.396	0.396	26.722	Time	0.155	0.261	26.151
Dosage	5.874	11.784	81.314	Dosage	- 2.649	- 2.233	- 109.052
% Solid^2	0.005	0.005	-0.016	% Solid^2	0.006	0.005	-
pH^2	2.841	1.819	30.899	pH^2	-	-	-
Time^2	- 0.008	-0.010	0.153	Time^2	-	-	0.164
Dosage^2	- 0.127	-0.447	24.537	Dosage^2	-	-	16.631
% Solid * pH	- 0.050	-0.243	2.599	% Solid * pH	-	- 0.292	1.806
% Solid * Time	0.006	0.0001	-0.004	% Solid * Time	-	-	-
% Solid * Dosage	0.135	0.146	-0.402	% Solid * Dosage	0.134	0.151	-
pH * Time	- 0.084	0.005	-5.040	pH * Time	-	-	- 4.331
pH * Dosage	- 1.165	-1.385	-34.214	pH * Dosage	-	-	-
Time * Dosage	0.066	0.014	0.936	Time * Dosage	-	-	-
R	0.9663	0.9713	0.9767	R	0.9231	0.9567	0.9559
Adj.R^2	0.9301	0.9405	0.9496	Adj.R^2	0.9056	0.9415	0.9362

5.6. Conclusions

We discussed the dissolution capacity of metal ions from kaolin particles in the absence and presence of three different anionic dispersing agents. In kaolin structure, the edge is only the positively charged sites at the experimental conditions. The edge is mostly dominated by alumina and the positively charged aluminum ion sites is ($AlOH_2^+$) in the solution. Its functional group is ($-OH_2^+$). Adsorption takes place between the positively charged sites of aluminum and negatively charged part of dispersing agents due to electrostatic and electrosteric attraction and produces soluble complex ions. NaHMP produced more dissolved aluminum ions than NaPAA and Na-Silicate. When dispersing agent is used, the pH of the suspension was around 5 for NaHMP, 6.5 for NaPAA and 8.5 or 9 for Na-Silicate. If the pH of the suspension is low, the adsorption of dispersing agents onto the alumina surface is increasing. On the other hand, there are more places for the adsorption. If the adsorption is more, complex ion formation is also more. Therefore, NaHMP produced more dissolved aluminum ions and then NaPAA and Na-Silicate respectively.

In summary, the dissolution capacities of metal ions from crude kaolin particles strongly depend on the type of the dispersing agents and the pH condition of the suspension.

CHAPTER 6
SUMMARY AND CONCLUSIONS

In Chapter 1, three common disinfection methods were discussed and their advantages and disadvantages were explained. Chlorination is the most common disinfection method for wastewater today, but as an alternative method, Ultraviolet (UV) and ozone disinfection techniques are developing.

In Chapter 2, Odometric transformation and the method of characteristics were explained. An odemetric transformation replaces time with β in the model and transforms the dynamics of the system to a constant time delay model. The advantage of new variable β is to obtain the model as a constant delay, which is equal to the length of the contact basin. Constant delay increases control performance. In this chapter, Method of Characteristics method used to transform the partial differential equations of the model to the ordinary differential equations.

In Chapter 3, Cascade control and Dead-time compensation strategies were explained. A cascade control scheme involves a slave loop and a master loop. The probe of the slave controller is located near the chlorine dosage point. Since the delay is too small, it can be tuned efficiently. The other controller is the master controller that adjusts the set point of the slave controller. The master is affected by a large and variable dead time. However, using an odometric transformation, the reactor model can be written as a constant dead time system. The Smith Predictor is then used to design an effective dead-time compensation for the master controller.

In Chapter 4, Cascade control and Dead-Time Compensation strategies were applied with an odometric transformation to control the chlorine disinfection of wastewater. The maximum numbers of reactor and control variables were calculated using the open loop simulation program. Delays were calculated for each system and the highest delay was calculated when the numbers of reactor was the maximum. This delay was close to the delay that calculated using an odometric transformation. It was the total length of contact basin. When Δt was 20, the sable response was observed for the system.

In Chapter 5, the effect of pH and three different anionic dispersants (sodium polyacrylate, sodium hexametaphosphate and sodium silicate) were investigated on the dissolution capacity of metal ions from kaolin particles. The dosage of dispersing agent, pH, solid concentration and aging significantly affected solubility of metal ion concentrations. The amount of released aluminum and silicon ions increased with increasing the dosage of any dispersant. Sodium hexametaphosphate produced the highest amount of aluminum ions in the suspension and then sodium polyacrylate and sodium silicate followed. The solubility of metal ions was also affected by the pH of the suspension. Released aluminum ions precipitated as $Al(OH)_3$ with increasing and decreasing the pH of the suspension and the concentration of soluble aluminum decreased in the suspension. In the same way, increasing the pH of the suspension results the formation of aluminosilicate surface on the silica surface of particles and this situation prohibited the release of silicon ions from the kaolin particles. Some of aluminum ions adsorbed onto the surface of released silicon ions and formed alumino-silicate gel. Formation of alumino-silicate gel decreased the concentration of soluble silicon ions.

CHAPTER 7
SUGGESTIONS FOR FUTURE WORK

To date all our experiments have been carried out at the Kanapaha Water Reclamation Facility (KWRF) and the University of Florida wastewater treatment plant (UP) and our simulation studies are based on the dimensions of these plants's reactor for chlorine disinfection. Simulation results show that the odometric transformation and the application of the method of characteristics to solve the PDEs are adequate tools. The disinfection process at the UP is almost the same as at KWRF. The University plant has one contact basin and its capacity is lower than KWRF's basin. One advantage of working at the UP is that, in contrast to the KWRF, sensors are available for the measurement of ammonia concentration. If the inlet ammonia concentration can be measured accurately, complete chlorine disinfection models would be able to applied for the entire reactor. This would allow developing a comprehensive model-based control strategy for the wastewater treatment plant.

In summary, suggested proposed experimental work involves taking extensive new measurements as a function of time of the following variables.

- Chlorine concentration at the dosing point and secondary probe.
- Ammonia concentration at the basin inlet, and the volumetric flow rate of the inlet wastewater stream.

These measurements will then be used to produce accurate models for the UP and to design advanced controller.

A cascade/ratio controller currently controls the disinfection process and gives good results at KWRF. The outlet chlorine concentration is approximately between 2.5 and 3 mg/L, which is close to the target value of 1 mg/L. However, a large and varying dead time is still the main problem preventing better approaches to the target value. The flow rate changes significantly between day and night time. As a result, chlorine demand also varies widely. Improved performance is desired.

The implementation of the controller can be done using the Wanderware software interface available at the UP. The research work will involve the using of the controllers under Wanderware protocols, and the tuning of the slave and master controller.

A predictive control scheme can also be investigated and compared with the cascade/ratio controller.

Adsorption mechanism of dispersing agents onto the kaolin surface was almost identified and all experiments were conducted in ERC(Particle Science and Technology of Engineering Research Center). The pH of the suspension, dosage, solid concentration and aging showed that they had significant effects on solubility of aluminum and silicon ions. Using the DOE software, complete and best models were developed for the dissolution of aluminum and silicon ions from the particles. These models can lead to design a pH controller and keep the properties of suspensions at the desired conditions. Using a controller can also control rheological properties of the dispersion. Viscosity can be measured automatically during the process and can be adjusted to the minimum value by manipulating the dispersant dosage.

APPENDIX A
SIMULATION PROGRAM FOR ODOMETRIC TRANSFORMATION USING MATLAB

Program Name: Reactor_run.m

```
This program makes the reactor.m program run and plots the results
clear
tic;

%Physical parameters
Z1 = 76.5                    %Length of 1st basin [m]
Z2 = 46.4                    %Length of pipe [m]
Z3 = 113.386                 %Length of 2nd basin [m]
Z  = Z1+Z2+Z3                %Total Length

%Integration Limits
sigma_o      = 0             %Initial place
sigma_f_1    = sqrt(2)*Z1    %Upper limit for reactor 1
sigma_f_2    = sqrt(2)*Z2    %Upper limit for reactor 2
sigma_f_3    = sqrt(2)*Z3    %Upper limit for reactor 3

%Integration parameters
SIGMASPAN_1      = [sigma_o sigma_f_1]
SIGMASPAN_2      = [sigma_o sigma_f_2]
SIGMASPAN_3      = [sigma_o sigma_f_3]
OPTIONS          = []

Delta_t      = 1             %time increment [sec]

t_o          = 200           %initial time [sec]
t_f          = 500           %final time [sec]

c_ext_sol    = []
t_int        = []
D_1_sol      = []
D_2_sol      = []
D_3_sol      = []
D_total_sol  = []
t_ext_sol    = []
```

```
% Extract concentration at the end of the reactor
f_HOCL      = 52.3 *1000  %[mg/mol]
f           = [f_HOCL]'

% Initial conditions
% IN TERMS OF [ppm]
% HOCL_o    = ?           %Initial conditions
% NH3_3     = 0           %Initial conditions
% NH2CL_o   = 0
% NHCL2_o   = 0
% NCL3_o    = 0
% NOH_o     = 0
% NO3_o     = 0
% N2_o      = 0

% Experimental Data
% Data

Data1;    % Data file from Kanapaha 01/27/1999
t_exp_1             = Data_reac_1(:,1)          %Time [min]

beta_exp_1          = Data_reac_1(:,8)
vel_exp_1           = Data_reac_1(:,7)          %Velocity to [meter/min]
HOCL_final_exp_1    = Data_reac_1(:,5)
HOCL_exp_1          = Data_reac_1(:,4)          %Conc. of HOCL [g/liter]
CL2_dosage          = Data_reac_1(:,2)
HOCL_exp_1_         = Data_reac_1(:,4)/(52.3*1000) %Conc. of HOCL [mol/liter]
clear Data_reac_1

Data2     % Data file from Kanapaha 01/27/1999
t_exp_2             = Data_reac_2(:,1)          %Time [min]
beta_exp_2          = Data_reac_2(:,8)
vel_exp_2           = Data_reac_2(:,7)          %Velocity [meter/sec]
clear Data_reac_2

Data_3    % Data file from Kanapaha 9/1/1998
t_exp_3             = Data_reac_3(:,1)          %Time [min]
beta_exp_3          = Data_reac_3(:,8)
vel_exp_3           = Data_reac_3(:,7)          %Velocity [meter/min]
clear Data_reac_3

% Post message to the screen
dips('******* Reactor_run ********')

% Integrate over time
for   t = t_o : Delta_t : t_f
```

```
% Display time on the screen for every Delta_t
      msg = sprintf(' t = %g min',t) ; disp(msg)

% ********** For first reactor *************

beta_o_1      = interp1(t_exp_1,beta_exp_1,t,'linear')
HOCL_o_1      = interp1(beta_exp_1,HOCL_exp_1_,beta_o_1,'linear')
x0_1          = [HOCL_o_1]

% Integrate over sigma
[sigma_1,x_1] = ode45('reactor1',SIGMASPAN_1,x0_1,OPTIONS,
                      beta_exp_   1,vel_exp_1,beta_o_1,Z1)
beta_current_1 = beta_o_1 + sigma_f_1/sqrt(2)
t1             = interp1(beta_exp_1, t_exp_1, beta_current_1, 'linear')

% ********** For Second Reactor *************

beta_o_2      = interp1(t_exp_2,beta_exp_2,t1,'linear')
x0_2          = x_1(end,:)

% Integrate over sigma
[sigma_2,x_2] = ode45('reactor2',SIGMASPAN_2,x0_2,OPTIONS,
                      beta_exp_2,vel_exp_2,beta_o_2,Z2)
% Calculate beta_o and beta_current
beta_current_2 = beta_o_2 + sigma_f_2/sqrt(2)
t2             = interp1(beta_exp_2, t_exp_2, beta_current_2, 'linear')

% ********** For Third Reactor *************

beta_o_3      = interp1(t_exp_3,beta_exp_3,t2,'linear')
x0_3          = x_2(end,:)

% Integrate over sigma
[sigma_3,x_3] = ode45('reactor3',SIGMASPAN_3,x0_3,OPTIONS,
      beta_exp_3,vel_exp_3,beta_o_3,Z3)

% Extract concentration at the end of the reactor
c_sol_3       = x_3(end,:)

% Calculate beta_o and beta_current
beta_current_3 = beta_o_3 + sigma_f_3/sqrt(2)
t3             = interp1(beta_exp_3, t_exp_3, beta_current_3, 'linear')

% Conc. of c_sol_3 is the effluent concentration at time t3
% Total delay is t3-t
% Solution of the simulation
```

```
c_ext_sol       = [c_ext_sol ; x_3(end,:)*f]
t_int           = [t_int ; t]
t_ext_sol       = [t_ext_sol ; t3]
end

Simulation_results = [t_int t_ext_sol (t_ext_sol-t_int)  c_ext_sol]
disp('Time_in(min) Time_ext(min) Delay(min)  HOCL_out [ppm]'); ...
        disp('---------- ---------- ---------- ----------'); ,  disp(Simulation_results);

% Plot results
plot(t_ext_sol,c_ext_sol,'o',t_exp_1,HOCL_exp_1,
        '-',t_exp_1,HOCL_final_exp_1)
AXIS([200 650 2 10])
grid
legend('Simulation Result','North Probe','Final Probe')
title(sprintf('Total Length = %g m',Z))
xlabel('t [min]')
ylabel('Concentration   [ppm]')
toc;
```

Program Name: Reactor1.m

```
function xdot_1 =
reactor1(sigma_1,x_1,FLAG,beta_exp_1,vel_exp_1,beta_o_1,Z1)
%function xdot = reactor(sigma,x,FLAG,beta_exp,vel_exp,beta,Z)

%Calculate beta_current
beta_current_1 = beta_o_1 + sigma_1/sqrt(2)

%Interpolate the value
if beta_current_1 <= 0
        v_1 = vel_exp_1(1)
        else
        v_1 = interp1(beta_exp_1, vel_exp_1, beta_current_1, 'linear')
end

%Calculate the derivatives
if isempty(FLAG)
        xdot_1  =  rxnrates1(x_1)/v_1/sqrt(2)
        else
        msg     =  sprintf(' FLAG = %g',FLAG);
        disp(msg);
        error('reactor called with non-empty flag')
end
```

Program Name: Reactor2.m

```
function xdot_2 =
reactor2(sigma_2,x_2,FLAG,beta_exp_2,vel_exp_2,beta_o_2,Z2)
%function xdot = reactor(sigma,x,FLAG,beta_exp,vel_exp,beta,Z)

%Calculate beta_o and beta_current
beta_current_2 =  beta_o_2 + sigma_2/sqrt(2)

%Interpolate the value
if beta_current_2 <= 0
        v_2 = vel_exp_2(1)
        else
        v_2 = interp1(beta_exp_2, vel_exp_2, beta_current_2,linear')
end

%Calculate the derivatives
if isempty(FLAG)
        xdot_2  =  rxnrates2(x_2)/v_2/sqrt(2)
        else
        msg     = sprintf(' FLAG = %g',FLAG)
        disp(msg)
        error('reactor called with non-empty flag')
end
```

Program Name: Reactor3.m

```
function xdot_3 =
reactor3(sigma_3,x_3,FLAG,beta_exp_3,vel_exp_3,beta_o_3,Z3)
%function xdot = reactor(sigma,x,FLAG,beta_exp,vel_exp,beta,Z)

%Calculate beta_o and beta_current
beta_current_3 =  beta_o_3 + sigma_3/sqrt(2)

%Interpolate the value
if beta_current_3 <= 0
        v_3 = vel_exp_3(1)
        else
        v_3 = interp1(beta_exp_3, vel_exp_3, beta_current_3,'linear')
end

%Calculate the derivatives
if isempty(FLAG)
        xdot_3 = rxnrates3(x_3)/v_3/sqrt(2)
        else
        msg     = sprintf(' FLAG = %g',FLAG);
        disp(msg);
        error('reactor called with non-empty flag')
end
```

Program Name: Rxnrates1.m

```
function r = rxnrates1(x_1)

%Fixed parameters
%H      = 1.122e-7          %H ion conc.          [mole/L]
%OH     = 8.913e-8          %OH ion conc.         [mole/L]
%n1     = 29.4118e-06       %inlet ammonia conc. [mole/L]
%HOCL= 180.952e-06          %HOCL ion conc.       [mole/L]
%R      = 0.00198           %Ideal Gas constant   [k-cal/ mole.K]
%Tk     = 288.15            %Temperature[K]
%pKa    = 7.632839          %Negative neparian logarithm

%Reactions Rate Constants
%RTk = R*Tk                          %[L.atm/mole ]
%k1   = 9.7e8  *  exp(-3/RTk)        %[L.(mole.sec)]
%k2   = 1.99e4 *  exp(-2.4/RTk)      %[L.(mole.sec)]
%k3   = 3.43e5 *  exp(-7/RTk)   * (1+(10^(-pKa+1.4))/H)  % [liter.(mole.sec)]
%k4   = 8.56e8 *  exp(-18/RTk)  * (1+5.88e5 * OH)
                                    %[1/sec]
%k5   = 2.03e14*  exp(-7.2/RTk) *  n1 * OH % [1/sec]
%k6   = 1e8    *  exp(-6/RTk)       %[L.(mole.sec)]
%k7   = 1.3e9  *  exp(-6/RTk)       %[L.(mole.sec)]
%k8   = 1e7    *  exp(-6/RTk)       %[L.(mole.sec)]
%k9   = 0.00135                     %[1/(mole.sec)]

%save kvec k1 k2 k3 k4 k5 k6 k7 k8 k9 w1 w2 n1 HOCL Tk R pKa H OH

%Species concentrations
 HOCL       = x_1
%NH3        = x (2)
%NH2CL      = x (3)
%NHCL2      = x (4)
%NCL3       = x (5)
%NOH        = x (6)
%NO3        = x (7)
%N2         = x (8)

%r_HOCL  = -k1 * HOCL * NH3-k2 * HOCL * NH2CL-k3 *   HOCL*NHCL2...;
%+ k4 * NCL3+k7 * NOH * NHCL2
%- 2 * k8 * HOCL * NOH -k_Slow*HOCL
%r_NH3   = -k1 * HOCL * NH3
%r_NH2CL =  k1 * HOCL * NH3 - k2 * HOCL * NH2CL
%- k6 * NH2CL * NOH
%r_NHCL2 =  k2 * HOCL * NH2CL - k3 * HOCL * NHCL2+k4*NCL3...;
%- k5 * NHCL2 - k7 * NOH * NHCL2
```

```
%r_NCL3  = k3 * HOCL * NHCL2 - k4 * NCL3
%r_NOH   = k5 * NHCL2 - k6 * NOH * NH2CL
%r_NO3   = k8 * NOH * HOCL
%r_N2    = k6 * NOH * NH2CL + k7 * NOH * NHCL2

%Reaction Rate Vector
k = 0.0072                    %Rate constant [1/h]
r_HOCL    = -k*HOCL

%r        = [r_HOCL ; r_NH3 ; r_NH2CL ; r_NHCL2 ; r_NCL3 ; r_NOH ; r_NO3 ;
            r_N2 ]
r         = [r_HOCL]
```

Program Name: Rxnrates2.m

```
function r = rxnrates1(x_2)

%Fixed parameters
%H      = 1.122e-7          %H ion conc.          [mole/L]
%OH     = 8.913e-8          %OH ion conc.         [mole/L]
%n1     = 29.4118e-06       %inlet ammonia conc.[mole/L]
%HOCL= 180.952e-06          %HOCL ion conc.       [mole/L]
%R      = 0.00198           %Ideal Gas constant   [k-cal/ mole.K]
%Tk     = 288.15            %Temperature          [K]
%pKa    = 7.632839          %Negative neparian logarithm

%Reactions Rate Constants
%RTk = R*Tk                          %[L.atm/mole ]
%k1   = 9.7e8  *  exp(-3/RTk)        %[L.(mole.sec)]
%k2   = 1.99e4 *  exp(-2.4/RTk)      %[L.(mole.sec)]
%k3   = 3.43e5 *  exp(-7/RTk)   * (1+(10^(-pKa+1.4))/H)
                                     %[liter.(mole.sec)]
%k4   = 8.56e8 *  exp(-18/RTk)  * (1+5.88e5 * OH)
                                     %[1/sec]
%k5   = 2.03e14*  exp(-7.2/RTk) *  n1 * OH   % [1/sec]
%k6   = 1e8    *  exp(-6/RTk)        %[L.(mole.sec)]
%k7   = 1.3e9  *  exp(-6/RTk)        %[L.(mole.sec)]
%k8   = 1e7    *  exp(-6/RTk)        %[L.(mole.sec)]
%k9   = 0.00135                      %[1/(mole.sec)]

%save kvec k1 k2 k3 k4 k5 k6 k7 k8 k9 w1 w2 n1 HOCL Tk R pKa H OH

%Species concentrations
 HOCL       = x_2
%NH3        = x (2)
%NH2CL      = x (3)
%NHCL2      = x (4)
%NCL3       = x (5)
%NOH        = x (6)
%NO3        = x (7)
%N2         = x (8)

%r_HOCL = -k1 * HOCL * NH3-k2 * HOCL * NH2CL-k3 *
%HOCL*NHCL2...;
%+ k4 * NCL3+k7 * NOH * NHCL2 ...
%-2 * k8 * HOCL * NOH –kslow*HOCL
%r_NH3 =  -k1 * HOCL * NH3
%r_NH2CL =  k1 * HOCL * NH3 - k2 * HOCL * NH2CL ...
%-k6 * NH2CL * NOH
```

```
%r_NHCL2 =  k2 * HOCL * NH2CL - k3 * HOCL *
%NHCL2+k4*NCL3...;
%-k5 * NHCL2 - k7 * NOH * NHCL2
%r_NCL3 =  k3 * HOCL * NHCL2 - k4 * NCL3
%r_NOH  =  k5 * NHCL2 - k6 * NOH * NH2CL
%r_NO3  =  k8 * NOH * HOCL
%r_N2   =  k6 * NOH * NH2CL + k7 * NOH * NHCL2

%Reaction Rate Vector
k = 0.0072                          %Rate constant [1/h]
r_HOCL   = -k*HOCL

%r          = [r_HOCL ; r_NH3 ; r_NH2CL ; r_NHCL2 ; r_NCL3 ; r_NOH ; r_NO3 ;
              r_N2 ]
r           = [r_HOCL]
```

Program Name: Rxnrates3.m

```
function r = rxnrates1(x_3)

%Fixed parameters
%H      = 1.122e-7          %H ion conc.          [mole/L]
%OH     = 8.913e-8          %OH ion conc.         [mole/L]
%n1     = 29.4118e-06       %Inlet ammonia conc.[mole/L]
%HOCL= 180.952e-06          %HOCL ion conc.       [mole/L]
%R      = 0.00198           %Ideal Gas constant   [k-cal/ mole.K]
%Tk     = 288.15            %Temperature          [K]
%pKa    = 7.632839          %Negative neparian logarithm

%Reactions Rate Constants
%RTk  = R*Tk                          %[L.atm/mole]
%k1   = 9.7e8  *  exp(-3/RTk)         %[L.(mole.sec)]
%k2   = 1.99e4 *  exp(-2.4/RTk)       %[L.(mole.sec)]
%k3   = 3.43e5 *  exp(-7/RTk)  * (1+(10^(-pKa+1.4))/H)
                                      %[liter.(mole.sec)]
%k4   = 8.56e8 *  exp(-18/RTk) * (1+5.88e5 * OH)%[1/sec]
%k5   = 2.03e14*  exp(-7.2/RTk) *  n1 * OH     %[1/sec]
%k6   = 1e8    *  exp(-6/RTk)         %[L.(mole.sec)]
%k7   = 1.3e9  *  exp(-6/RTk)         %[L.(mole.sec)]
%k8   = 1e7    *  exp(-6/RTk)         %[L.(mole.sec)]
%k9   = 0.00135                       %[1/(mole.sec)]

%save kvec k1 k2 k3 k4 k5 k6 k7 k8 k9 w1 w2 n1 HOCL Tk R pKa H OH

%Species concentrations
  HOCL      = x_3
%NH3        = x (2)
%NH2CL      = x (3)
%NHCL2      = x (4)
%NCL3       = x (5)
%NOH        = x (6)
%NO3        = x (7)
%N2         = x (8)

%r_HOCL  = -k1 * HOCL * NH3-k2 * HOCL * NH2CL-k3 * HOCL*NHCL2...;
%+ k4 * NCL3+k7 * NOH * NHCL2 ...
%- 2 * k8 * HOCL * NOH –kSlow* HOCL
%r_NH3    = -k1 * HOCL * NH3
%r_NH2CL  = k1 * HOCL * NH3 - k2 * HOCL * NH2CL ...
%- k6 * NH2CL * NOH
%r_NHCL2  = k2 * HOCL * NH2CL - k3 * HOCL * NHCL2+k4*NCL3...
%- k5 * NHCL2 - k7 * NOH * NHCL2
```

```
%r_NCL3   = k3 * HOCL * NHCL2 - k4 * NCL3
%r_NOH    = k5 * NHCL2 - k6 * NOH * NH2CL
%r_NO3    = k8 * NOH * HOCL
%r_N2     = k6 * NOH * NH2CL + k7 * NOH * NHCL2

%Reaction Rate Vector
 k              = 0.0072                                    %Rate constant [1/h]
 r_HOCL         = -k*HOCL

%r  = [r_HOCL ; r_NH3 ; r_NH2CL ; r_NHCL2 ; r_NCL3 ; r_NOH ; r_NO3 ; r_N2 ]
r         = [r_HOCL]
```

APPENDIX B
OPEN LOOP SIMULATION PROGRAM USING VISUAL BASIC

```
Option Explicit
Sub Dead_Time_Comp_Open_loop2()

Dim L As Single, V As Single, C_HOCLo As Single, C_HOCL As Single, Tav As
Single
Dim Tcal As Single, Kgain As Single, K As Single, Qo As Single, DbetaStar As Single
Dim Css As Single, Cspss As Single, Ii As Single, ykbeta As Single, Nreac As Single
Dim D As Single, n As Single, S As Single, t As Single, Dt As Single, Beta As Single
Dim Tfi As Single, Beta_zero As Single, Beta_store As Single, CSp2 As Single
Dim Csp1 As Single, ysp2 As Single, ykPrevious As Single, ebetaPrevious As Single
Dim ebeta2Previous As Single, Kc As Single, Tintegral As Single, Tderivative As Single
Dim Q As Single, Vvel As Single, y2beta As Single, y2betaStar As Single, ebeta As
Single
Dim PbetaPrevious As Single, Pbeta As Single, IAE As Single, ITAE As Single, Umax
As Single
Dim I As Long

'This program uses Dead_Time Compensation to calculate the set point of slave loop
'controller for chlorine disinfection process of Wastewater treatment plant

                '********** With Deviation Variables **********

'Physical parameters

L           = 97            'Length of the reactor (m)
C_HOCLo     = 4.5           'Inlet chlorine concentration  (ppm)  (North Probe)
C_HOCL      = 2.8           'Outlet chlorine concentration  (ppm)  (Final Probe)
Tav         = 0.58          'Average detention time (hr)
Tcal        = 22            'Model tau in beta units (m)
Kgain       = 0.6219        'Process Transfer function gain (Estimated)
K           = 0.000258      'Rate constant  ( (1/sec),  0.93 (1/hr))
Nreac       = 50            'Number of Reactors  (dimensionless)
V           = 146 / Nreac   'Volume of each reactor  (m^3, 5156 ft^3)
Qo          = 0.0793        'Flow rate (m^3/sec, 285.5 m^3/hr, 1.81 MGD, 10082.44
                            ft^3/hr)
D           = 64            Time delay obtained from open loop response curve
n           = 20
DbetaStar   = D / n         'Time increment  (m)
```

```
S           = 1.61      'Crossectional area (m^2)
t           = 0         'Initial time (hr)
Tfi         = 200000    'Final Time (sec)
Dt          = 20        'Time increment (sec)
Beta_zero   = 0         'Beta value which is at the beginning of the reactor
Beta        = 0
Beta_store  = 0
Css         = C_HOCL    'Steady state value of final probe
Cspss       = C_HOCLo   'Steady state value of north probe
CSp2        = 2.8       'Estimated operator set point value for final probe HOCL
                        (ppm)
Csp1        = Cspss
Ii          = 0         'Index for printing every time csp1 changes
IAE         = 0
ITAE        = 0
'Umax       = 10        ' Maximum possible dosage (ppm)

'Worksheet labeling

Cells(1, 1) = (" Time (sec) ")
Cells(1, 2) = (" Beta (m) ")
Cells(1, 3) = (" y2 (beta) final probe (ppm) ")
Cells(1, 4) = (" Flow rate Q (m^3/sec) ")
Cells(1, 5) = (" P (beta) Controller output ")
Cells(1, 6) = (" IAE Results ")
Cells(1, 7) = (" ITAE Results ")

'Initial values

ykbeta = C_HOCL                 'Estimated value HOCL (ppm)
ebetaPrevious = CSp2 - ykPrevious
ebeta2Previous = ebetaPrevious

'Calculation of PID controller using velocity form
'Tuning parameters
'Estimated controller parameters

Kc = 0
Tintegral = 100
Tderivative = 0

10

Dim j As Integer
Dim U(20) As Single             'Note: Dimension should be equal to n
Dim C(5000), F(5000) As Single  'Note: Dimension should be equal to Nreac
```

```
'Initialization of input U

For I = 0 To n - 1
        U(I) = 0
Next I

'Initialization of initial north probe concentrations (ppm)

For I = 1 To Nreac
        C(I) = C_HOCLo
Next I

'Updating new beta and time
'Beginning of simulation loop

For I = 0 To Tfi Step 1
Q = Qo + 0.8 * Qo * Sin(2 * 3.14159 * t / 24 / 60 / 60)
Vvel = Q / S

'Step Change part, if it is needed

If t > 4000 Then Csp1 = C_HOCLo + 0.2
t = t + 1
Beta = Beta + Vvel * Dt

'Calculation of Derivatives using Euler Method

F(1) = Q / V * (Csp1 - C(1)) - K * C(1)

For j = 2 To Nreac
        F(j) = Q / V * (C(j - 1) - C(j)) - K * C(j)
Next j

For j = 1 To Nreac
        C(j) = C(j) + Dt * F(j)
Next j

If Beta - Beta_store < DbetaStar Then GoTo 20

'Update beta, y2beta, and ykbeta

Beta_store = Beta
y2beta = C(Nreac) - Css

'Calculation of ykbeta
```

```
ykbeta = (1 - DbetaStar / Tcal) * ykbeta + Kgain * (U(0) - U(n)) * DbetaStar / Tcal
ykPrevious = ykbeta

40

'Calculation of y2betaStar

y2betaStar = y2beta + ykbeta

50

'Error calculation e(beta)

ebeta2Previous = ebetaPrevious
ebetaPrevious = ebeta
ebeta = (CSp2 - Css) - y2betaStar

'IAE and ITAE results
IAE = Abs(ebeta) * Dt + IAE
ITAE = Abs(ebeta * t) * Dt + ITAE

60

'Calculation of output of controller Pbeta

PbetaPrevious = U(0)
Pbeta = ebeta - ebetaPrevious + DbetaStar / Tintegral * ebeta
Pbeta = Pbeta + Tderivative / DbetaStar * (ebeta - 2 * ebetaPrevious + ebeta2Previous)
Pbeta = PbetaPrevious + Kc * Pbeta

'Addition of saturation limits

'If Pbeta < 0 Then Pbeta = 0
'If Pbeta > Umax Then Pbeta = Umax

70

'Update the push-down stack

For j = n To 1 Step -1
        U(j) = U(j - 1)
Next j

U(0) = Pbeta
Csp1 = U(0) + Cspss
```

```
Cells(2 + Ii, 1).Value = t
Cells(2 + Ii, 2).Value = Beta
Cells(2 + Ii, 3).Value = y2beta
Cells(2 + Ii, 4).Value = Q
Cells(2 + Ii, 5).Value = U(2)
Cells(2 + Ii, 6).Value = IAE
Cells(2 + Ii, 7).Value = ITAE
Ii = Ii + 1

20

Next I

End Sub
```

APPENDIX C
CLOSED LOOP SIMULATION PROGRAM USING VISUAL BASIC

```
Option Explicit
Sub Dead_Time_Comp_Close_loop1()

Dim L As Single, V As Single, C_HOCLo As Single, C_HOCL As Single, Tav As
Single
Dim Tcal As Single, Kgain As Single, K As Single, Qo As Single, DbetaStar As Single
Dim Css As Single, Cspss As Single, Ii As Single, ykbeta As Single, Nreac As Single
Dim D As Single, n As Single, S As Single, t As Single, Dt As Single, Beta As Single
Dim Tfi As Single, Beta_zero As Single, Beta_store As Single, CSp2 As Single
Dim Csp1 As Single, ysp2 As Single, ykPrevious As Single, ebetaPrevious As Single
Dim ebeta2Previous As Single, Kc As Single, Tintegral As Single, Tderivative As Single
Dim Q As Single, Vvel As Single, y2beta As Single, y2betaStar As Single, ebeta As
Single
Dim PbetaPrevious As Single, Pbeta As Single, IAE As Single, ITAE As Single, Umax
As Single
Dim I As Long

'This program uses Dead_Time Compensation to calculate the set point of slave loop
'controller for chlorine disinfection process of Wastewater treatment plant
'Physical parameters

                '********** With Deviation Variables **************

L           = 97          'Length of the reactor (m)
C_HOCLo     = 4.5         'Inlet chlorine concentration  (ppm)  (North Probe)
C_HOCL      = 2.8         'Outlet chlorine concentration  (ppm)  (Final Probe)
Tav         = 0.58        'Average detention time (hr)
Tcal        = 22          'Model tau in beta units (m)
Kgain       = 0.062314    'Process Transfer function gain (Estimated)
K           = 0.000258    'Rate constant ( (1/sec),  0.93 (1/hr))
Nreac       = 50          'Number of Reactors  (dimensionless)
V           = 146 / Nreac 'Volume of each reactor  (m^3, 5156 ft^3)
Qo          = 0.0793      'Flow rate (m^3/sec, 285.5 m^3/hr, 1.81 MGD,
                          10082.44 ft^3/hr)
D           = 79          'Time delay obtained from open loop response curve
n           = 10
DbetaStar   = D / n       'Time increment  (m)
S           = 1.61        'Crossectional area (m^2)
```

```
t           = 0          'Initial time (hr)
Tfi         = 120000     'Final Time (sec)
Dt          = 20         'Time increment (sec)
Beta_zero   = 0          'Beta value which is at the beginning of the reactor
Beta        = 0
Beta_store  = 0
Css         = C_HOCL     'Steady state value of final probe
Cspss       = C_HOCLo    'Steady state value of north probe
CSp2        = 2.8        'Estimated operator set point value for final probe HOCL
                         (ppm)
Csp1        = Cspss
Ii          = 0          'Index for printing every time csp1 changes
IAE         = 0
ITAE        = 0
'Umax       = 10         'Maximum possible dosage (ppm)

'Worksheet labeling

Cells(1, 1) = (" Time (sec) ")
Cells(1, 2) = (" Beta (m) ")
Cells(1, 3) = (" y2 (beta) final probe (ppm) ")
Cells(1, 4) = (" Flow rate Q (m^3/sec) ")
Cells(1, 5) = (" P (beta) Controller output ")
Cells(1, 6) = (" IAE Results ")
Cells(1, 7) = (" ITAE Results ")

'Initial values
ykbeta = C_HOCL                    'Estimated value HOCL (ppm)

ebetaPrevious = CSp2 - ykPrevious
ebeta2Previous = ebetaPrevious

'Calculation of PID controller using velocity form
'Tuning parameters
'Estimated controller parameters

Kc = 0.5
Tintegral = 100
Tderivative = 0

10

Dim j As Integer
Dim U(20) As Single                'Note: Dimension should be equal to n
Dim C(10000), F(10000) As Single   'Note: Dimension should be equal to Nreac
```

```
'Initialization of input U

For I = 0 To n - 1
        U(I) = 0
Next I

'Initialization of initial north probe concentrations (ppm)

For I = 1 To Nreac
        C(I) = C_HOCLo
Next I

'Updating new beta and time
'Beginning of simulation loop

For I = 0 To Tfi Step 1
Q = Qo + 0.8 * Qo * Sin(2 * 3.14159 * t / 24 / 60 / 60)
Vvel = Q / S
t = t + 1
Beta = Beta + Vvel * Dt

'Calculation of Derivatives using Euler Method

F(1) = Q / V * (Csp1 - C(1)) - K * C(1)

For j = 2 To Nreac
        F(j) = Q / V * (C(j - 1) - C(j)) - K * C(j)
Next j

For j = 1 To Nreac
        C(j) = C(j) + Dt * F(j)
Next j

If Beta - Beta_store < DbetaStar Then GoTo 20

'Update beta, y2beta, and ykbeta

Beta_store = Beta
y2beta = C(Nreac) - Css

'Calculation of ykbeta

ykbeta = (1 - DbetaStar / Tcal) * ykbeta + Kgain * (U(0) - U(n)) * DbetaStar / Tcal
ykPrevious = ykbeta
```

```
'Calculation of y2betaStar

y2betaStar = y2beta + ykbeta

50

'Error calculation e(beta)

ebeta2Previous = ebetaPrevious
ebetaPrevious = ebeta
ebeta = (CSp2 - Css) - y2betaStar

'IAE and ITAE results

IAE = Abs(ebeta) * Dt + IAE
ITAE = Abs(ebeta * t) * Dt + ITAE

60

'Calculation of output of controller Pbeta

PbetaPrevious = U(0)
Pbeta = ebeta - ebetaPrevious + DbetaStar / Tintegral * ebeta
Pbeta = Pbeta + Tderivative / DbetaStar * (ebeta - 2 * ebetaPrevious + ebeta2Previous)
Pbeta = PbetaPrevious + Kc * Pbeta

'Addition of saturation limits

'If Pbeta < 0 Then Pbeta = 0
'If Pbeta > Umax Then Pbeta = Umax

70

'Update the push-down stack

For j = n To 1 Step -1
        U(j) = U(j - 1)
Next j

U(0) = Pbeta
Csp1 = U(0) + Cspss

Cells(2 + Ii, 1).Value = t
Cells(2 + Ii, 2).Value = Beta
Cells(2 + Ii, 3).Value = y2beta
Cells(2 + Ii, 4).Value = Q
```

```
Cells(2 + Ii, 5).Value = U(2)
Cells(2 + Ii, 6).Value = IAE
Cells(2 + Ii, 7).Value = ITAE
Ii = Ii + 1

20

Next I

End Sub
```

LIST OF REFERENCES

Anastassiadis, A., 1994. MS Thesis, Control Strategies of A Wastewater Chlorination Process With Variable Dead Time, University of Florida, Gainesville, Florida, U.S.A.

Chu, J., Su, H., Gao, F., and Wu, J., 1998. Process Control: Art or Practice, Annual Reviews in Control. Vol. 22, 59-72.

Devidal, J., Schott, J., and Dandurand, J., 1997. An experimental study of kaolinite dissolution and precipitation kinetics as a function of chemical affinity and solution composition at 150°C, 40 bars, and pH 2, 6, 8, and 7.8. Geochimi. Cosmochim. Acta. Vol. 61, No. 24, 5165-5186.

Ganor, J., Mogollan, J., L., and Lasaga, A., C., 1995. The effect of pH on kaolinite dissolution rates and on activation energy. Geochimi. Cosmochim. Acta. Vol. 59, No. 6, 1037-1052.

Grasso, D., 1996. Wastewater Disinfection, Water Environment Federation, 601 Wythe Street, Alexandria, Virginia, 40 pp.

Hammer, M.J., and Hammer, M.J. Jr., 1996. Water and Wastewater Technology, Third edition, Prentice-Hall, New Jersey. 252 pp.

Harmon, J., Pullammanappallil, P., Svoronos, S.A., Lyberatos, G., and Chynoweth, D. P., 1990. On-line identification of a variable sampling period discrete model and its use for the adaptive control of anaerobic digestion. Proceedings of the 1990 American Control Conference (IEEE Cat. No.90CH2896-9), Vol. 2, 1540-1545.

Herington, T.M., Clarke, A.Q., and Watts, J.C., 1992. The surface charge of kaolin. Colloids and Surfaces. Vol. 68, 161-169.

Holtzclaw, H. F., Robinson, W. R., and Odom, J. D., 1991. General Chemistry with Qualitative Analysis. 9nd ed., D. C. Heath and Company., Lexington, Massachusetts, 397 pp.

Huertas, F.J., Chou, L., and Wollast, R., 1998. Mechanism of kaolinite dissolution at room temperature and pressure: Part I. Surface speciation. Geochimi. Cosmochim. Acta. Vol. 62, No. 3, 417-431.

Huertas, F.J., Chou, L., and Wollast, R., 1999. Mechanism of kaolinite dissolution at room temperature and pressure: Part II. Kinetic study. Geochimi. Cosmochim. Acta. Vol. 63, No. 19/20, 3261-3275.

Iler, R.K., 1973. Effect of adsorbed alumina on the solubility of amorphous silica in water. J. Colloid Interface Sci. Vol. 43, 399-408.

Kendall, T., 1995. Kaolin competition intensifying. In: Bolger, R.L., O'Driscoll, M.J. (Eds.), Raw Materials for Pigments, Fillers and Extenders, Industrial Minerals, 79.

Konta, J., 1995. Clay and man: Clay raw materials in the service of man, Appl. Clay Sci., Vol. 10, 275-335.

Lau, P.J., 1997. Applying Disinfection Alternatives to Wastewater Treatment, Pollution Engineering Online.

Levine, W.S., 1996. The Control Handbook, CRC Press, Inc., IEEE Press, Inc., Massachusetts.

Mann, P.S., 1995. Introductory Statistics. 2nd ed., Jhon Wiley & Sons, inc., New York, 441 pp.

Marlin, T.E., 1995. Process Control-Designing Processes and Control Systems for Dynamic Performance, McGraw-Hill, Inc. New York.

McClave, J.T., Dietrich ll, F.H., and Sincich T., 1997. Statistics. 7th ed. Prentice Hall Inc. Simons & Schuster / A Viacom Company Upper Saddle River, New Jersey, 535 pp.

Mcmurry, J., and Fay, R. C., 1998. Chemistry. 2nd ed., Prentice-Hall, Inc., New Jersey, 670 pp.

Morris, J.C., and Wei, I.W., 1969. Chlorine Ammonia Breakpoint Reactions: Model Mechanisms and Computer Simulation, Am. Chem. Soc., Div. Water, Air and Waste Chem., Minneapolis, April 15.

Murray, H.H., 2000. Traditional and new applications for kaolin, smectite, and palygorskite: a general overview, Appl. Clay Sci., vol. 17, 207-221.

Okamoto, G., Okura, T., and Goto, K., 1957. Properties of silica in water, Geochimi. Cosmochim. Acta. Vol. 12, 123-132.

Ott, L., 1988. An Introduction to Statistical Methods and Data Analysis. PWS-Kent Publishing Co., Boston, 1988, Chaps. 12-13.

Reed, D., 1998. Selecting Alternatives to Chlorine Disinfection, Pollution Engineering Online, Magazine Articles.

Saunier, B. and Selleck, R.E., 1979. Ph.D. Thesis, Kinetics of Breakpoint Chlorination and Disinfection, University of California, Berkeley, California, U.S.A.

Seborg, D.E., Edgar, and T.F., Mellichamp, D.A., 1989. Process Dynamics and Control,Wiley and Sons, New York.

Sjoberg, M., Bergstrom, L., Larsson, A., and Sjostrom, E., 1999. The effect of polymer and surfactant adsorption on the colloidal stability and rheology of kaolin dispersion, J. Colloids and Surface Sci. Vol. 159, 197-208.

Stefanopoulos, G., 1984. Chemical Process Control, Prentice-Hall, Engelwood Cliffs, New Jersey.

Subramanian S., Santhiya D., Shanbhag S.B., Natarajan K.A., and Malghan S.G., in: Mehrotra S.P., Shekhar R. (Eds), 1995. Mineral Processing: Recent Advances and Future Trends, Allied Publishers. New Delhi, 45-52.

Svoronos, S.A., and Lyberatos, G., 1992. Eigenvalue-Based Method for Automatically Adjusting the Sampling Interval, AIChE J., Vol. 38, No. 9, 1485-1488.

Tchobanoglous, G., and Schroeder, E.D., 1985. Water Quality, Addision-Wesley Publishing Company, Massachusetts.

Weaver, C.E., and Pollard, L.D., 1973. The Chemistry of Clay Minerals, Elsevier Scientific Publishing Company, Amsterdam, London, New York, 130 pp.

Wefers, K., and Misra, C., 1987. Oxides and Hydroxides of Aluminum, Alcoa Laboratories. 3 pp.

Van Olphen, H., 1991. Clay Colloid Chemistry. 2nd ed. Krieger Publishing Company., Malabar, Florida, 29 pp.

Yuan, J., Garforth, W.L., and Pructt, R.J., 1998. Influence of dispersants on the solubility of calcined kaolin, Appl. Clay Sci., 13, 137-147.

BIOGRAPHICAL SKETCH

Feridun Demir was born in Gaziantep, Turkey, on February 25, 1968. He received his bachelor's degree in Chemical Engineering from Hacettepe University in August 1993 in Ankara, Turkey. After one year of work in industry in Turkey, he studied intensive English at the Middle East Technical University with a Turkish Government scholarship. He moved to the United States for graduate study. He went to Polytechnic University in Brooklyn, New York, where he earned a master's degree in Chemical Engineering in June 1997. In August 1997, he entered the Ph.D program in the Chemical Engineering Department at the University of Florida.

I certify that I have read this study and that in my opinion it conforms to acceptable standards of scholarly presentation and is fully adequate, in scope and quality, as a dissertation for the degree of Doctor of Philosophy.

Oscar D. Crisalle, Chairman
Associate Professor of Chemical Engineering

I certify that I have read this study and that in my opinion it conforms to acceptable standards of scholarly presentation and is fully adequate, in scope and quality, as a dissertation for the degree of Doctor of Philosophy.

Abbas A. Zaman, Cochairman
Assistant Engineer, Materials Science and Engineering

I certify that I have read this study and that in my opinion it conforms to acceptable standards of scholarly presentation and is fully adequate, in scope and quality, as a dissertation for the degree of Doctor of Philosophy.

Spyros A. Svoronos
Professor of Chemical Engineering

I certify that I have read this study and that in my opinion it conforms to acceptable standards of scholarly presentation and is fully adequate, in scope and quality, as a dissertation for the degree of Doctor of Philosophy.

Ben L. Koopman
Professor of Environmental Engineering Science

I certify that I have read this study and that in my opinion it conforms to acceptable standards of scholarly presentation and is fully adequate, in scope and quality, as a dissertation for the degree of Doctor of Philosophy.

Gar B. Hoflund
Professor of Chemical Engineering

This dissertation was submitted to the Graduate Faculty of the College of Engineering and to the Graduate School and was accepted as partial fulfillment of the requirements for the degree of Doctor of Philosophy.

December 2001

Pramod P. Khargonekar
Dean, College of Engineering

Winfred M. Phillips
Dean, Graduate School